2019

Evaluation of Helical Piles as Anchors for Floating Offshore Wind Turbine Foundation Systems

Martha Shannon Harris
University of Massachusetts Amherst

EVALUATION OF HELICAL PILES AS ANCHORS FOR FLOATING OFFSHORE WIND TURBINE FOUNDATION SYSTEMS

A Master Project Presented

By

Martha Shannon Harris

Master of Science in Civil Engineering

Department of Civil and Environmental Engineering University of Massachusetts

Amherst, MA 01003

FEBRUARY 2020

EVALUATION OF HELICAL PILES AS ANCHORS FOR FLOATING OFFSHORE WIND TURBINE FOUNDATION SYSTEMS

A Masters Project Presented

by

MARTHA SHANNON HARRIS

Approved as to style and content by:

Don J. DeGroot, Co-Chairperson

Sanjay R. Arwade, Co-Chairperson

Caitlyn Butler
Civil and Environmental Engineering Department

ACKNOWLEGEMENTS

I would like to extend my thanks and appreciation to the following people for their assistance to this project: Professor Don DeGroot, co-chair, advisor and mentor, for his guidance and support throughout this project; Professor Sanjay Arwade, for serving as a co-chair and for his assistance and advice; Professor Alan Lutenegger, Professor Charles Aubeny and Professor Michael Brown for their expertise and insight; for Casey Fontana, Krishnaveni Balakrishna, and my classmates for their help and support; for my friends and family for their endless encouragement.

ABSTRACT

EVALUATION OF HELICAL PILES AS ANCHORS FOR FLOATING OFFSHORE WIND TURBINE FOUNDATION SYSTEMS

FEBRUARY 2020

Martha Harris, B.S., University of Massachusetts Amherst

M.S., University of Massachusetts Amherst

Directed by Dr. Don J. DeGroot and Dr. Sanjay R. Arwade

The development of floating offshore wind energy is essential for growth of the renewable energy industry, and to decrease the reliance on fossil fuels and emission of greenhouse gasses. Advances in ease of construction and installation of turbines can make the floating offshore wind industry more marketable and feasible on a large scale; this can in part be achieved by innovation in foundation anchoring systems.

This thesis presents an evaluation of helical pile foundations for offshore deep-water application as anchors for floating offshore wind systems with catenary mooring lines in clay and sandy soils. This research outlines the influence of helical geometry, angle of installation and pile group effects on helical pile capacity and required installation torque. Axial capacities were determined using Terzaghi's general bearing capacity equations, lateral capacities were determined using American Petroleum Institute Recommended Practice and required installation torque was estimated using a Cone Penetration Test based system of equations. Models of semisubmersible and spar buoy floating offshore wind turbine platforms with single-line and multiline catenary mooring systems were used to generate expected anchor loads for design. Given the variance in functionality, both single piles and pile groups of four and nine were considered in

the analysis. Load conditions and pile configurations were compared to suction caissons and evaluated for efficiency and ease of construction.

The use of a spar buoy platform and multiline system decreased the required helical pile size compared to a semisubmersible platform and a single-line mooring system. Helical piles designed for sand were smaller in size compared to helical piles in clay due to greater strength of the sand. Individual helical piles designed for pile groups were smaller in overall geometry than single piles, where battered helical pile groups were lighter and vertical helical pile groups were heavier than single piles in terms of net weight. However, smaller helical piles required a fraction of the torque needed to install the larger, single helical piles. For efficiency in terms of capacity per unit weight, single and groups of helical piles are more efficient than suction caissons, using less steel to produce the same capacity. For catenary line systems the helix of a vertically installed helical pile does not contribute to lateral load resistance but it does provide a means for potentially quieter installation compared to driven piles.

TABLE OF CONTENTS

LIST OF TABLES

LIST OF FIGURES

LIST OF VARIABLES

Symbol:	Description:
A	stress drop index
aqc	radial stress
A	cyclic loading factor
A_H	effective helix area
A_S	shaft area
D	depth to helical plate
D_H	helix diameter
D_r	relative density
D_S	shaft diameter
C_1, C_2, C_3	coefficients determined by ϕ'
e_0	initial void ratio
Fr	friction ratio, CPT profile
F_S	side resistance
F_C	breakout factor
k	internal modulus of subgrade reaction force
K_0	earth pressure at rest
K_t	empirical correlation factor
K_{v0}	empirical correlation factor with void ratio
L	shaft length
N	number of helical piles
N_c	bearing capacity factor
N_q	bearing capacity factor

p	pitch
p_{ud}	lateral capacity, deep depths
p_{us}	lateral capacity, shallow depths
P	lateral soil resistance
$Q_{compressive}$	compressive capacity
Q_H	bearing capacity from helical plate
$Q_{lateral}$	lateral capacity
Q_S	bearing capacity from shaft
Q_t	axial capacity from installation torque verification
Q_{ug}	pile group capacity
Q_{us}	single pile capacity
$Q_{ultimate}$	ultimate capacity
Q_{uplift}	uplift capacity
R_s	settlement ratio
s_u	undrained shear strength
S_g	settlement ratio of pile group center
S_s	settlement ratio of single pile
S_t	sensitivity
t_H	helical plate thickness
t_S	shaft thickness
T	installation torque
T_b	installation torque from base of pile shaft
T_h	installation torque from helical plate

T_{h1}	friction on the underside of helical plate
T_{h2}	friction on the outside edge of helical plate
T_{h3}	friction on the leading edge of helical plate
T_s	installation torque from pile shaft area
w	water content
W	weight
X	depth
y	lateral deflection
α	batter angle
α^*	adhesion factor
β	mooring force rotation angle from direction of batter
γ'	effective unit weight
γ_t	total unit weight
δ_{crit}	soil-steel interface friction angle
Δx	interval of length
η_g	reduction in ultimate group capacity
θ	pitch angle
ν	Poisson's ratio
σ'_{v0}	vertical effective stress
ϕ'	friction angle
ϕ'_{cv}	constant volume friction angle
ϕ'_{crit}	critical state friction angle
ψ	angle of dilation

CHAPTER 1: INTRODUCTION

1.1 Introduction

Wind turbines turn kinetic energy from wind into mechanical power to generate electricity. While becoming more common on land and in shallow offshore waters, there is motivation to install wind turbines farther offshore to harness energy from stronger ocean winds and generate more power. Installation in deeper waters allows for larger turbines with higher megawatt capabilities but requires augmentation to the traditional fixed-bottom support structures used to support the wind turbine.

A floating wind turbine system consists of a platform tethered in place with mooring lines and anchors; this is a popular design type with a range of platform geometries, mooring line configurations, and anchor types being explored (Fontana 2019). Little research has been conducted for the use of helical piles as the anchor for these floating platforms. Traditionally light weight and simple to install in comparison to traditional anchoring methods for terrestrial and shallow offshore applications, there is interest in the potential use of helical piles as an anchoring system for floating offshore wind turbines. Since helical piles can also support multidirectional loading, they hold potential for multiline mooring systems.

The goal of this research was to design and evaluate helical pile foundations in an offshore environment to determine the practicality and feasibility of using helical piles as anchors for floating offshore wind turbine platforms.

1.2 Objectives and Scope of Research

The primary objective of this research was to study helical piles under loading conditions from models of semisubmersible and spar buoy floating offshore wind platforms with single-line and multiline catenary mooring systems in clay and sandy soil.

The scope of this research included the design and evaluation of helical pile foundations under four load conditions in two soil types and included the following tasks:

1. Design and capacity calculation of a single helical pile installed vertically
2. Design and capacity calculation of a group of four helical piles in a 2x2 square layout installed vertically
3. Design and capacity calculation of a group of four helical piles in a 2x2 square layout installed with a 25° batter
4. Design and capacity calculation of a group of nine helical piles in a 3x3 square layout, installed vertically
5. Design and capacity calculation of a group of nine helical piles in a 3x3 square layout, installed with a 25° batter
6. Design and capacity calculation of uniformly battered and radially battered group of helical piles in a 2x2 layout installed with a 25° batter
7. Estimation of required installation torque for piles and pile groups installed in sandy soil using a CPT based prediction method (Davidson et al. 2018)

1.3 Thesis Organization

Chapter 2 presents a brief literature review on floating offshore wind turbine foundation systems and helical pile design. Topics include an overview of the floating offshore wind industry

and types of platforms, mooring systems and anchors being researched. This chapter also presents a short history, current applications, limitations and methods of installations of helical piles.

Chapter 3 presents the methods of analysis, which include environmental and loading conditions, helical pile design considerations, axial and lateral capacity calculations using variations of Terzaghi's general bearing capacity equations and American Petroleum Institute Recommended Practice, and estimation methods for required installation torque using a Cone Penetration Test based system of equations.

Chapter 4 is divided into four sections. Section 4.1 presents design results for a single helical pile installed vertically in clay and sandy soil, and comparisons of this foundation method to another foundation type, suction caissons, in deep water application. Section 4.2 presents design results for pile groups, positioned in a square layout of 2x2 or 3x3 and installed vertically or with a 25° batter in the soil. This section compares the use of single piles versus pile groups and evaluates the effects of battered helical pile groups. Section 4.3 presents a comparison of uniformly battered and radially battered helical pile groups under rotated loading conditions. Section 4.4 presents required installation torque for single helical piles and individual helical pile groups installed in sand and evaluates feasibility of installation.

CHAPTER 2: BACKGROUND

This chapter presents a brief summary of background information and prior research on floating offshore wind turbines and helical pile design. Topics include an overview of the floating offshore wind industry and types of platforms, mooring systems and anchors being researched for the industry. This chapter also presents a short history, current applications, limitations and installation methods of helical piles.

2.1 Floating Offshore Wind

2.1.1 Industry

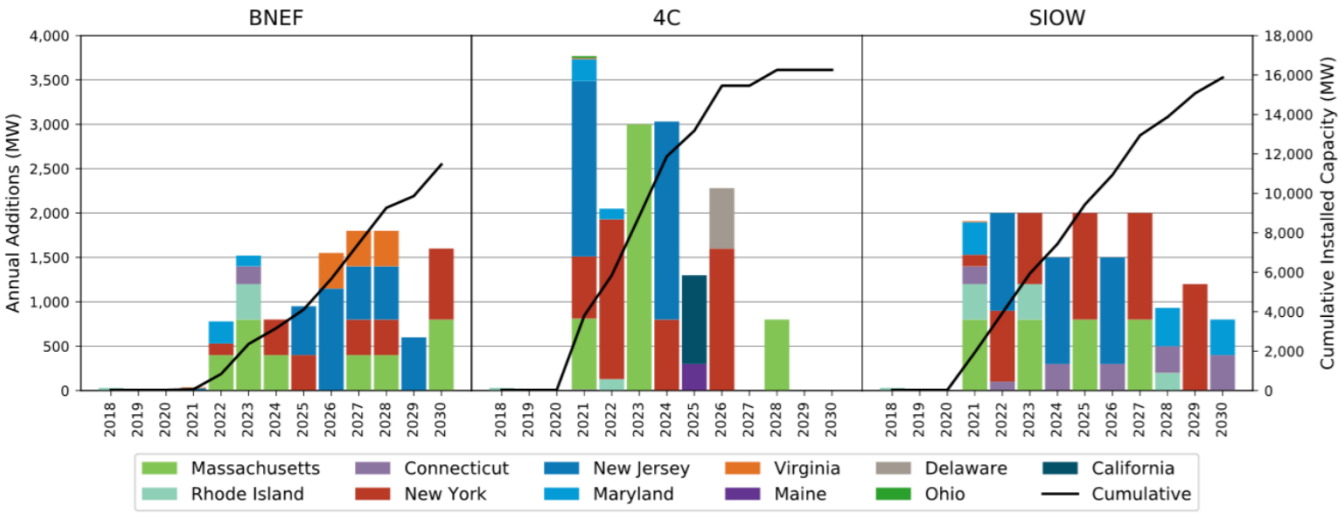

Figure 2.1. U.S offshore wind market forecasts for annual additions (left axis) and cumulative capacity (right axis) through 2030 (US Department of Energy 2019).

Offshore wind energy is a rapidly expanding industry that creates electricity by utilizing the natural convection of air over oceans with the use of turbines installed in coastal waters on fixed-bottom or anchored floating structures. In the United States in 2018, the overall size of the offshore wind energy project development and operational pipeline grew to a potential generating

capacity of 25.8 gigawatts (GW). The industry is predicted to grow its offshore wind capacity, shown in Figure 2.1. Plans for development of offshore wind activity was historically concentrated in East Coast states since its start in the 1990s, but has since spread to Pacific states, the Great Lakes and the Texas Gulf Coast due to state-level policy commitments and increased market interest. Competitive auctions for offshore wind leases in the U.S. and increased sale prices in 2018 indicate confidence and support from the market and from regulatory and financial institutions (US Department of Energy 2019).

Heightened interest and demand for offshore wind results in selection of activity sites and call areas in deeper coastal waters as shown in Figure 2.2. Activity in deeper water indicates a push towards floating platform technology, where larger turbines can generate more energy from stronger, more constant offshore winds.

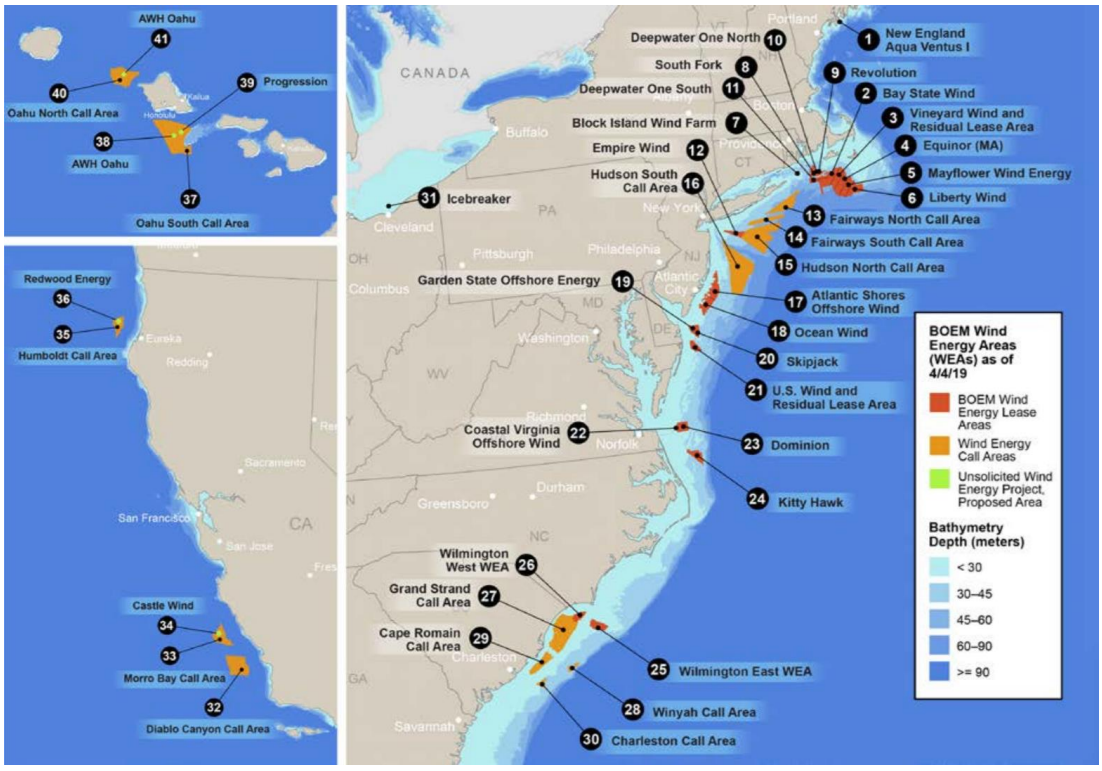

Figure 2.2 Locations of U.S. offshore wind pipeline activity and Call Areas as of March 2019 (US Department of Energy 2019).

2.1.2 Platforms

A floating offshore wind turbine (FOWT) consists of a buoyant platform secured to anchors with a system of mooring lines. Figure 2.3 shows some examples of FOWT platform types including buoyancy stabilized semisubmersibles, ballast-stabilized spar buoys and mooring stabilized tension leg platforms (Fontana 2019). Some semisubmersible platforms distribute water as an active ballast between the hull's columns to counteract thrust from wind and waves (e.g., Principle Power). Spar buoy platforms are steel cylinders filled with water, iron ore, or rock ballast to offset the weight of the wind turbine (Turkel 2019).

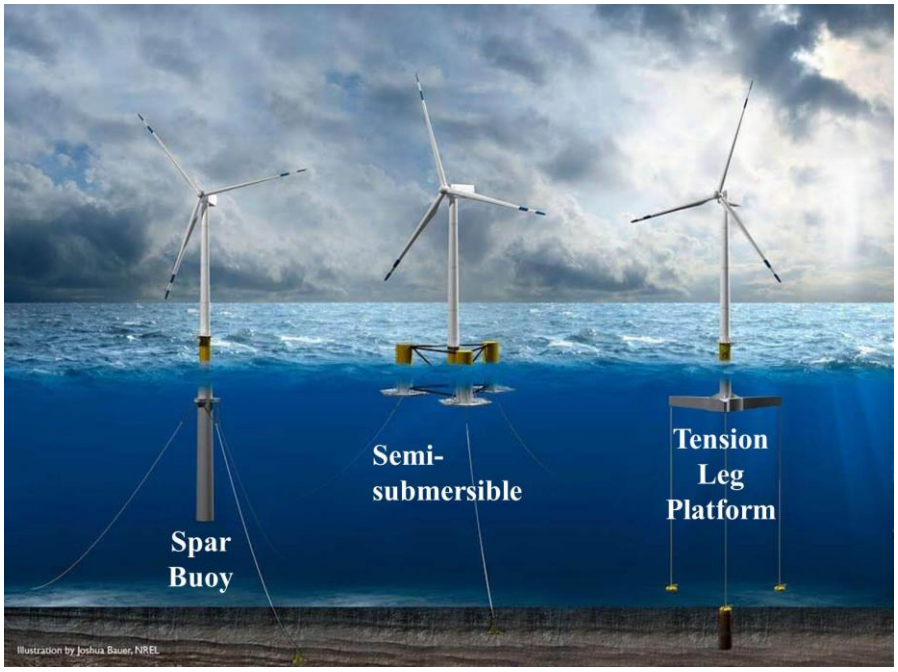

Figure 2.3. Floating Offshore Wind Platform Types (Fontana 2019).

2.1.3 Mooring and Anchor Systems

Mooring lines are typically composed of a combination of chain, wire rope, or fiber rope (API 2005). Mooring lines are connected to a joint on the floating platform, then hang in the water column in a catenary, semi-taut or taut design and are secured to anchors installed into the sea or

lakebed. Tension leg platforms use taut mooring lines while semisubmersible and spar buoy platforms can use semi-taut or catenary mooring lines.

A wide range of anchor types exist, including driven piles, suction caissons, dead weight and drag embedment anchors as illustrated in Figure 2.4. Anchor selection and design is determined based on water depth, angle of mooring line connection, soil conditions and other considerations like cost (Fontana & Hallowell 2018).

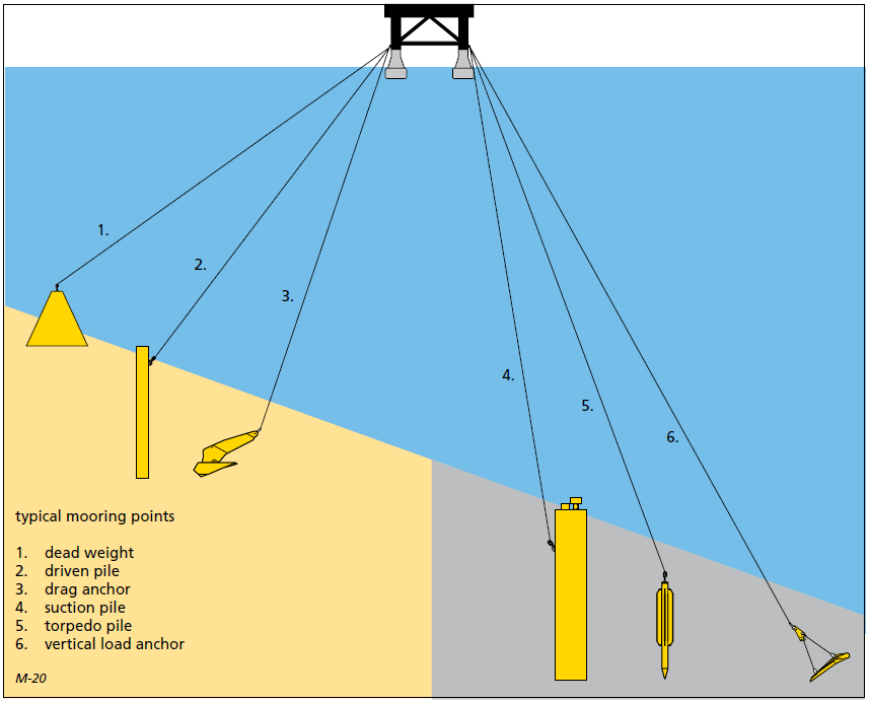

Figure 2.4. Anchor Types for Floating Offshore Wind Platforms (Vryhof 2010).

2.1.4 Multi-line Systems

One of the biggest obstacles in FOWT growth is optimizing the large platforms and foundation system to be more cost effective, as an estimated 36% of the total cost of an operating turbine comes from the construction and installation of the foundation and substructure, as depicted in Figure 2.5. Reducing this cost will make FOWT more competitive in the green alternative energy market (IREA 2016).

The multiline anchor concept is one method aimed to reduce foundation cost. For a single-line anchor concept, each FOWT is connected to the seafloor with at least 3 individual mooring lines and anchors. For a multiline concept, the turbine layout is designed to allow anchor sharing, where mooring lines from multiple FOWT connect to a single anchor. This reduces the number of required anchors and therefore reduces materials, installation and other costs for the anchor system (Fontana 2019).

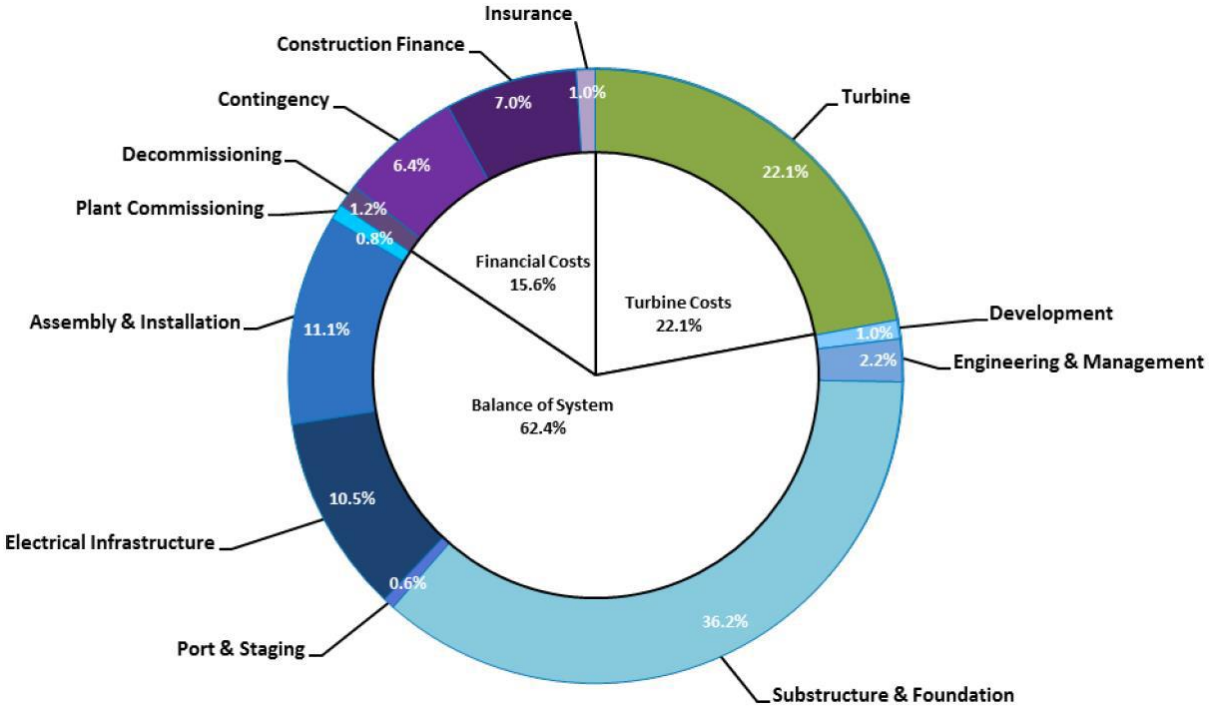

Figure 2.5. Breakdown of Capital Expenditures for the Floating Offshore Reference Wind Plant Project (Mone et al. 2015).

2.2 Helical Piles

A helical pile is a steel foundation pile with a central shaft with one or more helical bearing plates (DFI). Helical piles were historically used in shallow offshore applications and hold the potential to be cost effective as anchors to FOWT applications. Helical piles are not traditionally considered for deep water conditions, which can be attributed to an unknown method of installation in this environment, or perhaps disbelief that helical piles manufactured to comparable capacity of

existing anchors considered for FOWT would be effective. However, the simple and quiet installation method should make helical piles suitable for FOWT foundation systems.

2.2.1 History and Historical Applications

Helical piles were originally invented in the 1830s by Alexander Mitchell, the blind and self-described civil engineer. Mitchell was motivated to create a better way to safely moor ships in harbors and construct foundations for lighthouses in shallow water. Mitchell deemed that current piles and mooring methods could not generate enough holding power and upward strain resistance. The initial design consisted of an iron bar with a helical plate attached to the lower end that would be thrust into the soil with limited disturbance to resist downward pressure and upward strain (Lutenegger 2011). An example of an early helical pile design is shown in Figure 2.6.

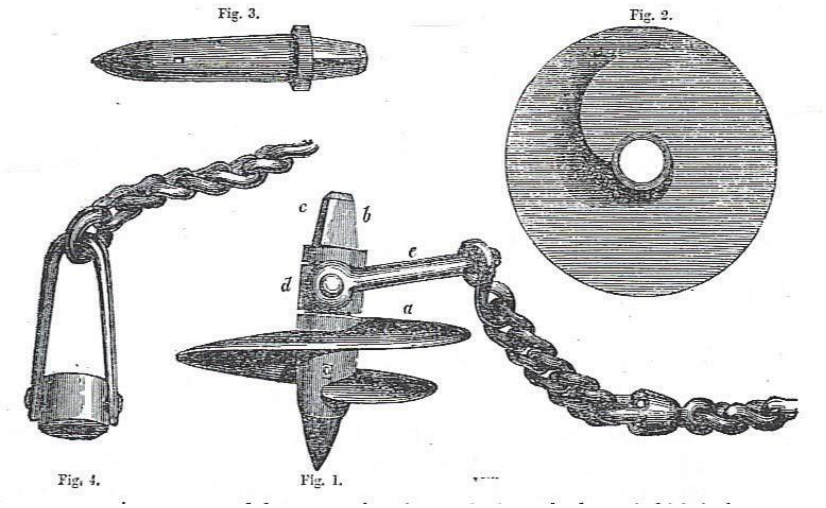

Figure 2.6. Sketch of Historical Helical Pile. H (Lutenegger 2017).

Helical piles were first used as a foundation element in 1838 for the Malpin Sands Lighthouse (Figure 2.7), where 9 helical piles, with a 5-inch shaft diameter and 4-foot helix, were installed 15 feet into sand by hand in open water. The project was well documented by Mitchell and included site investigations, field testing and proper observation during installation. The

successful performance of the Malpin Sands Lighthouse and other early helical pile lighthouse foundations influenced the U.S. Army Corps of Engineers to construct more than sixty lighthouses with helical pile foundations along the U.S. eastern coast by 1880 (Lutenegger 2011).

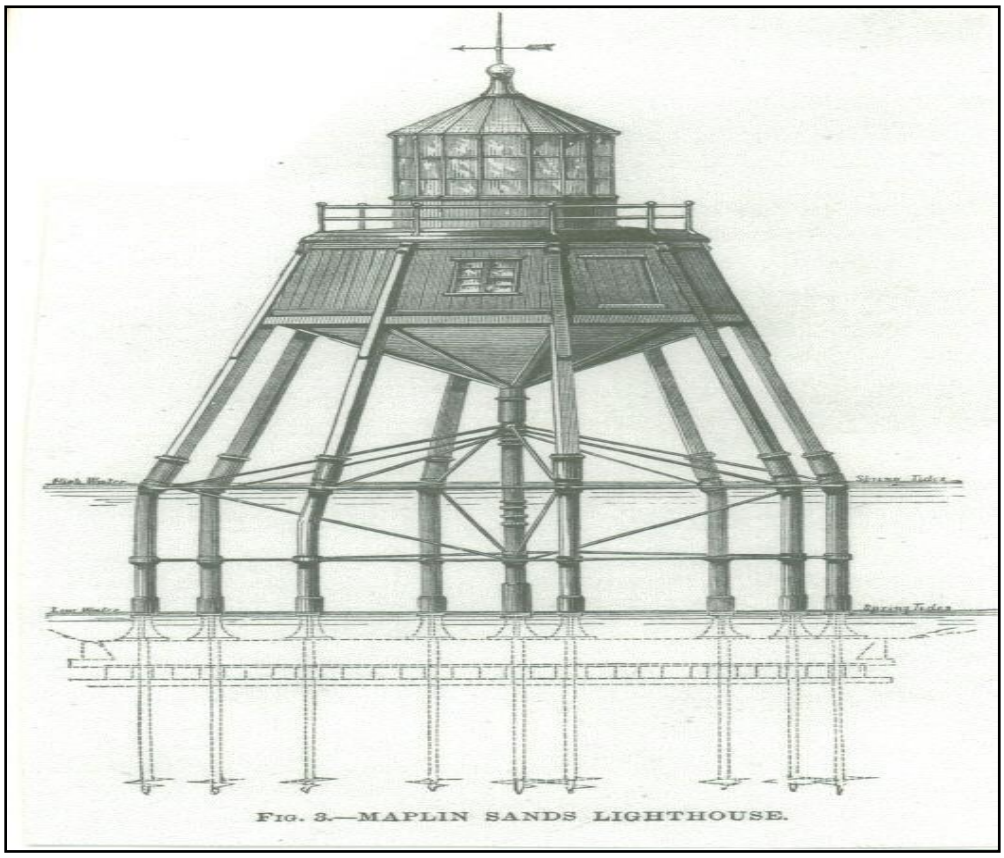

Figure 2.7. Mitchell's Malpin Sands Lighthouse Drawing (DFI 2019).

Mitchell broadened his work with helical piles and used them for coastal pier construction. In 1847, the pier extension in Courtown, Wexford proved that helical piles could be used to effectively support ocean front piers with efficient installation time and cost savings. Mitchell's work inspired other pier builders to use helical piles through the end of the 19th century in Europe, South America, India and the U.S. (Lutnegger 2011).

After the use of helical piles in pier construction grew, I.K. Brunel incorporated helical piles into bridge foundations. For a bridge across the Wye River in Chepstow, Wales, Brunel

designed 3-foot cast-iron cylinders with 12-inch helical flanches to drive 58 feet into the ground along the riverbed. By the late 1800s, many bridges were constructed using helical piles as the foundation. At this time, helical piles were also being used for underpinning old structures and as anchors to resist tensile loads in retaining walls and tunnel sections (Lutenegger 2011).

The geometry of helical piles evolved over time as technology advanced and engineers were finding new applications. Over time helical piles maintained a slender shaft and helical bearing plate, but changes in shaft and plate proportions were made for different projects; large, often hollow, round shafts with smaller helical plates for bearing, and solid square shafts with larger helical plates for anchors. After 1875, a large variety of helical piles existed for the ease of installation in different ground conditions, and multiple helices were added to increase capacity (Lutenegger 2011).

With development of other foundation methods and pile driving in the early twentieth century, the use of helical piles decreased. It was not until after World War II that helical pile usage increased again, with innovation of high capacity torque motors and the need to quickly rebuild bridges and buildings (DFI 2019).

2.2.2 Modern Applications

Advances in manufacturing technology have resulted in more efficient helical pile shape and size, and installation equipment. Today, helical piles are used for underpinning in foundation repair, new construction foundations, earth retention like tiebacks and helical soil nails, tie-downs, guy anchors and other applications (DFI 2019). An illustration of modern applications is shown in Figure 2.8.

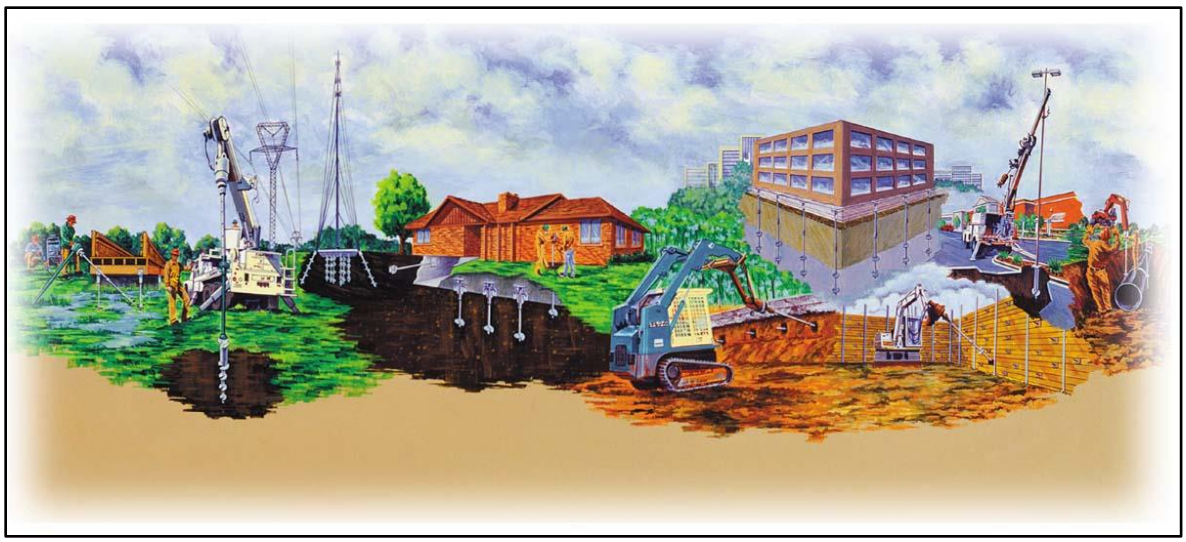

Figure 2.8. Illustration of Modern Helical Pile Application (DFI 2019).

With an increased need for alternative foundations, helical piles prove to be a competitive solution. Small central shafts and segmented sections make helical piles easy and inexpensive to mobilize. They can also be installed in a large variety of soil types and in year-round weather conditions. Relatively small installation equipment allows for helical piles to be installed in confined spaces with minimal noise and soil disturbance, which makes them advantageous for remedial and temporary work (DFI 2019).

2.2.3 Limitations

Helical piles also have some possible disadvantages. Because of the slim shaft and relatively small crowd, or downward force applied during installation, helical piles are unable to penetrate bedrock without pre-drilling. Similarly, helical piles can face refusal in soils with high cobble and boulder content and are difficult to install in solid waste fill containing concrete and other building debris. Slender shafts also limit lateral capacity, but augmentations can be made to increase this. DFI recommends a Factor of Safety of 2 be applied to the ultimate or working

capacity of the designed pile/foundation, which can be lowered where extensive testing is required and allows for it; a FS of 1.5 is common (DFI 2019).

2.3 Helical Pile Groups

A group of helical piles may be more suitable in some applications over a single helical pile, or another foundation type. Groups of smaller helical piles could be easier to transport and install with smaller equipment over a single helical pile of equivalent area, or helical plate area. There are also instances where a helical pile groups can be more economical than a single pile in regard to constructed unit load capacity per cost (Lutenegger 2018).

Little research has been done on the behavior of groups of helical piles, however some past studies have shown that the group performance changes from that of a simple summation of the performance of a single pile.. The overlapping of stress and strain fields of neighboring piles can cause a reduction in net performance for the group, which is often evaluated by the group efficiency and performance behavior (Lanyi-Bennett and Deng 2018). Group efficiency evaluates the reduction in ultimate group capacity, defined as (Whitaker 1957):

$$\eta_g = \frac{Q_{ug}/N}{Q_{us}} \quad (1)$$

where Q_{ug} is the capacity of the pile group, N is the number of piles in the group and Q_{us} is the capacity of a single pile. The numerator is called the average group capacity (Lanyi-Bennett and Deng 2018). Performance behavior is based on settlement, where the settlement ratio (R_s) is evaluated as the settlement of a pile group center (S_g) over the settlement of a single pile (S_s), as (Poulos and Davis 1980):

$$R_s = \frac{S_g}{S_s} \quad (2)$$

Limited studies of groups of plated piles in sand suggest a minimum shaft spacing of 3 to 4 times the diameter of the largest helical plate to avoid a group efficiency of less than 100% (DFI 2019). Experimental results for ultimate pullout load for pile groups in dense sand suggest a group efficiency exceeding 100% for pile groups of 6 and 9 piles spaced 3 and 4 helix diameters, and group efficiency of 100% or less for the same pile groups spaced 5 helix diameters (Hanna and Ghaly 1994). Group efficiencies greater than 100% can be attributed to the sand densifying during installation of closely spaced piles (Hanna and Ghaly 1994).

Uplift tests in stiff and soft clay of single-helix helical anchors installed in a 2x2 square determined that group efficiency varies with soil type and increases with pile spacing. Group efficiency was measured at displacement equal to 10% and 20% the pile diameter. For piles spaced 3 helix diameters, group efficiency was measured to be 91% to 96% in stiff clay and 138% to 141% in soft clay (Lutenegger 2018).

2.4 Helical Pile Installation

Helical piles are installed into soil using rotation, which requires torque to overcome frictional resistance at the soil-steel interface. Smaller surface area thus reduces the installation torque required. Estimating the required installation torque (T) is useful for choosing the appropriate machinery for the project and can be used to verify the axial capacity (Q_t) of the helical pile using an empirical correlation factor (K_t) and methods developed by Hoyt and Clemence (1989) using the equation as follows (Byrne and Houlsby 2015):

(3) $$Q_t = K_t T$$

Correlation factors have been empirically established based on load tests conducted in varying soil types over decades. Correlation factors are inversely related to shaft size; as helical

pile shaft increases, the K_t factor decreases (DFI 2019). K_t is not constant and can range from 10 to 66 m^{-1} depending on soil conditions, helix diameter, thickness and pitch, and load conditions (Perko 2009).

The British Standards, however, states that helical piles should not be designed only using empirical methods (British Standards Institution 2015). Alternative techniques of estimating the required installation torque have been developed. One method by Davidson et al. (2018), that improves on Al-Baghdadi et al. (2017), uses Cone Penetration Test (CPT) data to estimate installation torque in dense sand. Davidson et al. (2018) uses a system of equations to estimate the resulting total torque during installation with depth. The method relies on several factors including specific pile geometry, soil parameters and CPT friction ratio. Davidson et al. (2019) presents an updated version of this method

Methods of installation include use of a hydraulic torque drive that rotates the lead section into the ground. A torque indicator is attached to the drive tool to monitor the torque during installation. A hydraulic torque motor can be mounted to machines like front end skid-steer loaders, mini excavators and large excavators. Figure 2.9 shows helical pile installation with an excavator. Machines can also be secured to barges for shallow offshore installation. The installation is very quiet compared to other foundation types, like driven piles, which send pressure waves through the ground during installation. For sites with noise sensitivity, using helical piles over driven piles or other noisily installed foundation type. Helical piles can also be removed by torqueing in the opposite direction, which makes decommissioning structures with this foundation method simple and potentially quicker than other methods.

Figure 2.9. Example of Helical Pile Installation Process (DFI 2019).

Minimal research for deep water installation methods of helical piles have been published but is critical for helical pile application in water depths used in FOWT design. Limited research can be attributed to the large diameter of the helical piles needed for design loads that would require a hydraulic torque motor larger than any currently used in terrestrial installation. As installation torque is a function of pile geometry, decreasing the shaft and helical plate diameter would reduce the amount of torque needed for installation, but this would also reduce axial capacity, which is needed if load conditions are not perfectly perpendicular to the helical pile. Pile groups could be a potential solution to decreasing required installation torque but not sacrificing pile capacity. Another reason deep offshore installation of helical piles is limited is the lack of hardware. Currently there is not an effective commercial means of installation, be that a submersible drive head or a drive shaft stiff enough for installation in deep water.

CHAPTER 3: METHODS OF ANALYSIS

This chapter describes the methods used to design helical piles for this study. Loading conditions and soil conditions used for helical pile design are defined. Assumptions used for helical pile geometry are stated. Parameters and methods used in the calculation of lateral capacity using API Recommended Practice 2A-LRFD, ultimate capacity, uplift capacity and required installation torque are described.

3.1 Load Conditions

This section includes details of the environmental load conditions and design capacities used for helical pile foundation designs. In a previous study by Fontana (2019), single line and multiline geometries for FOWT were generated and evaluated for semi-submersible platforms for a 5MW turbine. Three mooring lines and anchors were used per FOWT. For the multiline system, each anchor secured three mooring lines, and for the single line system, each anchor secured one mooring line. Operating conditions were varied to evaluate the dynamics of the multiline anchor net force and single line anchor force. A similar study was conducted using identical operating conditions but for spar buoy platforms (K. Balakrishnan, personal communication, October 14, 2019). An example of a multiline system is illustrated in Figure 3.1.

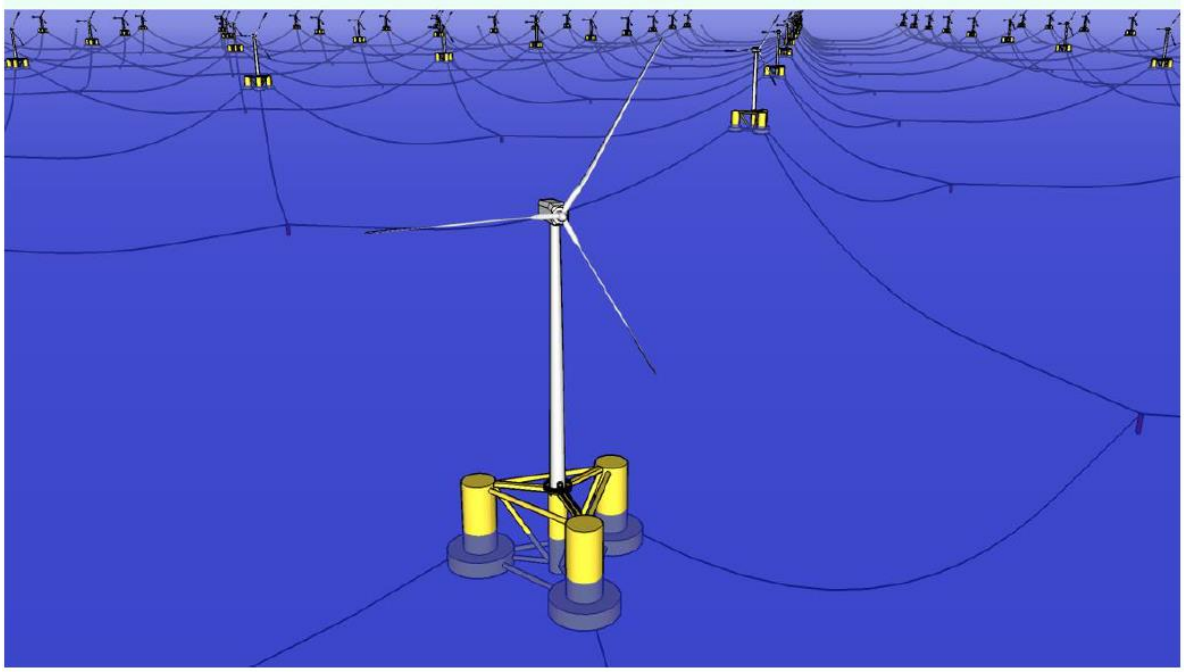

Figure 3.1. Multiline System for a Floating Offshore Wind Farm (Fontana 2019).

For this thesis, one set of operating conditions was chosen from these studies. The wind turbine "extreme" operating conditions for zero-degree wind, wave and current direction are specified in Table 3.1 (Fontana 2019).

Table 3.1. Details of Environmental Loading Condition (Fontana et al. 2017).

Condition	Extreme Operating (Strength)
Wind Speed at Hub Height	11.4 m/s (Rated)
Turbulence Intensity	10%
Significant Wave Height	8.0 m (50-yr)
Peak Spectral Wave Period	12.7 s
JONSWAP Gamma Factor	2
Current Speed	0.30 m/s
Water Depth	200 m
Mooring System	Catenary
Line Length	835.35 m (ss), 902.2 m (sb)
WWC	0°

Note: WWC refers to the angle of wind, wave and current direction
Note: "ss" refers Semisubmersible platform and "sb" refers to Spar Buoy platforms

Four loading conditions were chosen for this thesis, which consist of the maximum multiline net anchor force and maximum single line anchor force for both semisubmersible and spar buoy platforms. The modeled maximum net and single anchor forces are shown in Table 3.2. An industry-common factor of safety of 2 was applied to the maximum anchor forces and shown in Table 3.3. The maximum anchor force is applied at the ground surface to the top of the helical pile.

Table 3.2. Maximum Single-line and Multiline Anchor Net Forces for Semisubmersible and Spar Buoy Platforms in kN (Fontana et al. 2017).

Semi Submersible		Spar Buoy	
Multi-Line	Single-Line	Multi-Line	Single-Line
2151	2560	684	1444

Table 3.3. Maximum Single-line and Multiline Anchor Net Forces for Semisubmersible and Spar Buoy Platforms in kN – With F.S. = 2.

Semi Submersible		Spar Buoy	
Multi-Line	Single-Line	Multi-Line	Single-Line
4302	5120	1368	2888

3.2 Soil Conditions

This section describes the two soil conditions used for helical pile design. Both soil profiles were developed for this study, where the sand was developed to represent a medium-dense offshore sand deposit, and the clay was developed to be broadly representative of a soft offshore clay deposit. The soil properties of the medium-dense sand and soft clay are presented in Table 3.4 and Table 3.5. Note that for the soft clay, the undrained shear strength profile developed from the direct simple shear test was used in lateral and axial capacity calculations. Both soils were assumed to have no thixotropic behavior.

Table 3.4. Soil Properties of Medium-Dense Sand.

Depth z	m	0 to 35
Sediment	-	Med-dense sand
γ_t	kN/m^3	21
σ'_{v0}	kPa	10.9z
w	%	19
e_0	-	0.5
D_R	%	70
ϕ'	°	38
ϕ'_{crit}	°	33
δ_{crit}	°	27
ψ	°	11
ϕ'_{cv}	°	35
k_{v0}	m/s	3x10^{-5}
ν	-	0.3

Note: γ_w = 10.1 kN/m^3

Table 3.5. Soil Properties of Soft Clay.

Depth z	m	0 to 35
Sediment	-	Pleistocene CH/CL
γ_t	kN/m^3	17.4
σ'_{v0}	kPa	7.30z
s_u(DSS)	kPa	1.4 + 1.61z
s_u(TC)	kPa	2.0 + 2.34z
s_u(TE)	kPa	1.1 + 1.31z
S_t	-	6

Note: s_u(DSS) profile was used for lateral and axial capacity calculations

3.3 Single Helical Piles

This section describes the methods used to design a single helical pile installed vertically in soil, illustrated in Figure 3.2, which include pile geometry, lateral capacity calculation methods and axial capacity calculation methods.

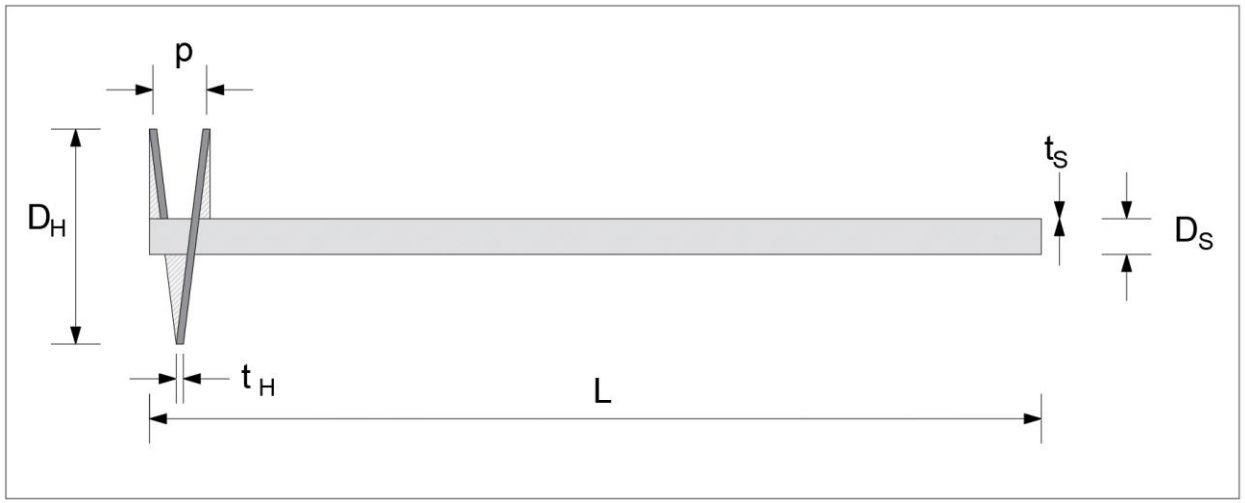

Figure 3.2. Helical Pile Schematic – To Scale.

3.3.1 Pile Geometry

The geometry of the helical piles designed in this study uses average proportions of central shaft length, shaft diameter, helix diameter, pitch and thickness from common industry sizes, shown in Table 3.6 and Figure 3.3. Pile length is solved for using lateral capacity equations. The ratio of shaft length (L) to central shaft diameter (D_S) and D_S to the helix diameter (D_H) is determined from Hubbell Power Systems CHANCE and Magnum Piling round shaft helical pile inventory. Shaft thickness used an API equation used for conservative design (API 1993). The pile is designed with a round shaft, which implies that shaft resistance is included in the axial capacity calculations. The pile is also designed with a closed end to eliminate possible plugging. The helix component consists of a single helical plate located at the end of the pile shaft. Helix pitch and thickness are chosen from Hubbell Power Systems CHANCE round shaft helical pile inventory. Note that shaft rotation is not considered in this study because pile shaft geometry is considered to be flexible with a length/diameter (L/D) greater than 1/8. If the L/D is equal to or less than 1/8 then rotation would need to be considered. For simplicity, the helical piles are designed so that no extension sections are needed after the helical pile lead section.

Table 3.6. Single Pile Geometry Proportions.

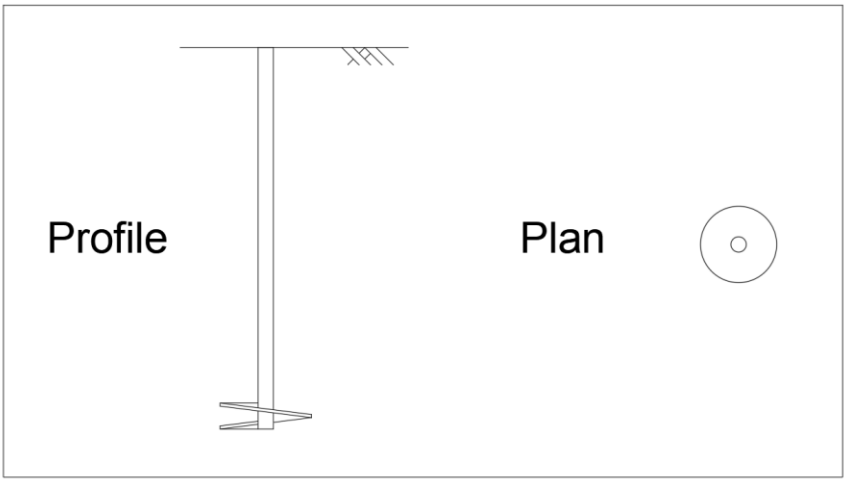

Figure 3.3. Single Helical Pile Profile and Plan View.

Vertical helical piles are compared with vertical suction caissons designed for the same four load conditions in medium dense sand and soft clay. The suction caissons were designed with a $L/D_S = 3$ and wall thickness of $t = D_S/144$ (Fontana 2019). The geometry of the suction caissons were found using the same methods for determining lateral capacity as the helical piles. Axial capacity was not calculated for suction caissons.

3.3.2 Lateral Capacity

Lateral resistance of the soil near the ground surface is crucial for piles that experience sustained lateral loads. For the design of helical piles, which have a relatively low lateral capacity compared to axial, and applying load strictly from the horizontal, the lateral resistance becomes the limiting capacity for design, or the allowable mooring force the helical pile can resist. For each load condition, the allowable mooring force was determined from the maximum net and single anchor forces. For vertical helical piles, the design lateral capacity is equal to the allowable mooring force. For helical piles installed with a positive batter, which is done for pile groups in

this study, the design lateral force is equal to allowable mooring force multiplied by the cosine of the batter angle.

American Petroleum Institute (API) procedure for finding lateral bearing capacity was used for pipe piles, assuming the lateral capacity generated from the helical plate was negligible. Lateral capacity for sand has been found to vary with depth, so the minimum of the lateral capacity for shallow depths (p_{us}) and the lateral capacity for deep depths (p_{ud}) should be used as the ultimate lateral bearing capacity ($Q_{lateral}$). For sand, equations 4 and 5 were used to determine lateral bearing capacity ($Q_{lateral}$) with depth.

(4) $$p_{us} = (C_1 X + C_2 D_s)\, \gamma' X$$

(5) $$p_{ud} = C_3 D_s \gamma' X$$

where γ' is effective weight of sand, X is depth, D_s is the pile shaft diameter, C_1, C_2 and C_3 are coefficients determined from figures in the API literature using the internal friction angle, ϕ'. The nonlinear lateral soil-deflection (p-y) relationship was approximated using the following equation.

(6) $$P = A\, Q_{lateral} \tanh \left[\frac{k\, X}{A\, Q_{lateral}} y\right]$$

where A is a factor to account for cyclic loading, k is the initial modulus of subgrade reaction force determined from a figure in the API literature using the internal friction angle, ϕ', y is lateral deflection and P is the lateral soil resistance.

For soft clay, lateral bearing capacity was determined using a variation of the API equations and the nonlinear lateral p-y relationship was a generated using a table specified in the API literature (API 1993). For both sand and clay soils, pile length varied in the API method to solve for the lateral capacity equal to the allowable mooring force for each load case. The pile length

and following geometry that resulted in the design lateral capacity is presented in Chapter 4 and was used for the axial capacity calculations.

3.3.3 Axial Capacity

After the pile length was solved for, the resulting pile geometry was used for the ultimate and uplift capacity calculations. For the ultimate and uplift capacity in both soils, no additional reduction factor was added for soil disturbance due an assumption of perfect installation, or "wished-in-place".

3.3.3.1 Ultimate Capacity

In sand, ultimate capacity was obtained using an effective stress analysis using the following equations developed by Terzaghi (Lutenegger 2019).

(7) $$Q_{ultimate} = Q_H + Q_S$$

(8) $$Q_H = A_H(\sigma'_{vo} N_q)$$

(9) $$Q_S = A_S F_S$$

(10) $$N_q = 0.5\ (12\varphi')^{\varphi'/54}$$

(11) $$F_S = \alpha^*\ \sigma'_{vo}$$

where the ultimate bearing capacity, $Q_{ultimate}$, is the sum of the ultimate capacity from the helix, Q_H, and the shaft resistance, Q_S. A_H is the effective area of the helical plate, or πD_H^2, and σ'_{v0} is the vertical effective stress of the sand at the depth of the helix, or $\gamma' D$, where D is the depth of the helical plate below the ground surface and γ' is the effective unit weight of the soil. The bearing capacity factor N_q of 37.2 was found using equation 10, where ϕ' is the internal friction angle. A_S

is the area of the shaft, or $\pi D_S L$, where L is the length of the central shaft. F_S is unit side resistance, which for sand is determined as the vertical effective stress at the depth of embedment times a reduction factor, α*. For this study α* was estimated to be a conservative value of 0.35 (U.S. Navy Design Manual 1986).

In clay, the ultimate capacity was also obtained using equation 7, but the ultimate bearing capacity (Q_H) is found using a total stress analysis and undrained shear strength in equation 12 where N_C is the bearing capacity factor, s_u is the undrained shear strength at the depth of the helix and γ is the total unit weight of the clay. A reduction of 25% is made to account for a moderately sensitive clay.

(12) $$Q_H = [A_H(N_c)s_u + \gamma D]0.75$$

(13) $$N_c = 6.0(1 + 0.2\ D/D_H) \leq 9$$

(14) $$F_S = \alpha^* s_u$$

Equation 9 is used to find shaft resistance, but unit side resistance for clay is found using an empirical adhesion factor, α* and s_u at mid pile shown in equation 14. The adhesion factor was determined using suggested values in Lutenegger (2019) assuming undisturbed conditions after the helical pile is installed and undrained loading.

3.3.3.2 Uplift Capacity

In sand, the uplift capacity is calculated using equations 7 through 11, except the effective area of the helical plate (A_H) changes to the cross-sectional area minus the area of the shaft, or $\pi D_H^2 - \pi D_S^2$.

In clay, the uplift capacity is calculated similar to the ultimate capacity, as shown in equation 15. F_C is a breakout factor solved for using equation 13. Like in sand, the effective area of the helical plate (A_H) changes to πD_H^2 - πD_S^2. The s_u is calculated slightly shallower than for ultimate, at the depth of the helix minus one helical plate diameter. The same reduction of 25% is applied for a moderately sensitive soil.

(15) $$Q_H = [A_H(F_c)s_u + \gamma D]0.75$$

3.4 Helical Pile Groups

This section includes the methods used to design helical pile groups of identical piles installed vertically and with a 25-degree batter in soil. This section includes additional pile geometry and layout considerations, and additional factors to lateral and axial capacity calculation methods.

The pile geometry assumptions stated in Section 3.3.1 are the same for pile groups. Shown in Figure 3.4, the helical piles are set up in a square configuration, of 2x2 or 3x3, and the shafts are spaced a length 4 times the helical diameter. This spacing was chosen so a group efficiency equal to 100% or 1 would be reasonable to assume for both the medium-dense sand and soft clay soils. For groups with piles installed at a batter, 25 degrees was chosen and was applied for calculations in both soils for consistency. A 25-degree batter was found to have the highest pullout capability for pile groups in sandy soil when compared to vertical piles and piles with batter angles of 20, 30, and 35 degrees from vertical (Singh and Arora 2017).

Table 3.7 presents the above layout assumptions. The battering is oriented in a positive direction or tilting towards the direction of the mooring line for all piles. This configuration was chosen for simplicity and to directly compare battered groups with vertically installed groups.

Table 3.7. Pile Group Geometry Proportions.

Pile Proportions		
Shaft Length	L	
Shaft Diameter	D_S	L/25
Helix Diameter	D_H	L/5
Helix Pitch	p	0.3 D_H
Helix Thickness	t_H	0.04 D_H
Shaft Thickness	t_S	0.00635+D_s/100
Pile Spacing	-	4D_H
Batter	degrees	25

For simplicity, it is assumed that each pile in the group receives equal pull from the mooring line. Since group efficiency was assumed to be 100%, the allowable mooring force per pile is equal to the allowable mooring force divided by the number of piles in the group. The pile length for an individual pile in the group is then solved for using the same methods as the single pile, where the design lateral capacity is equal to the allowable mooring force per pile. For battered piles, the design lateral capacity is equal to the allowable mooring force per pile times the cosine of the batter angle.

The axial capacities for individual piles in groups is determined using the same methods as the single pile. Note that for a vertical pile the shaft length, L, and the depth to helical plate, D, are equal. For a battered pile the shaft length is the same and the depth to helical plate is now found as the shaft length times the cosine of the batter angle.

Battering individual piles in a group in different directions could be more effective in a multiline system but this was not explored in depth in this study. Battered helical pile groups could be applied in a multiline system by radially battering helical piles towards a central connection

point to account for a potential change in the direction of the mooring line force from changes in weather conditions. An analysis of radially battered piles compares a helical pile group of 2x2 battered in a uniform direction to a helical pile group of 2x2 battered radially. This analysis uses the resulting geometry, and axial and lateral capacities found for a semisubmersible platform with a multiline catenary mooring system. Trigonometric equations were used to determine the capacity of individual piles and pile groups for rotated loading conditions and batter orientation.

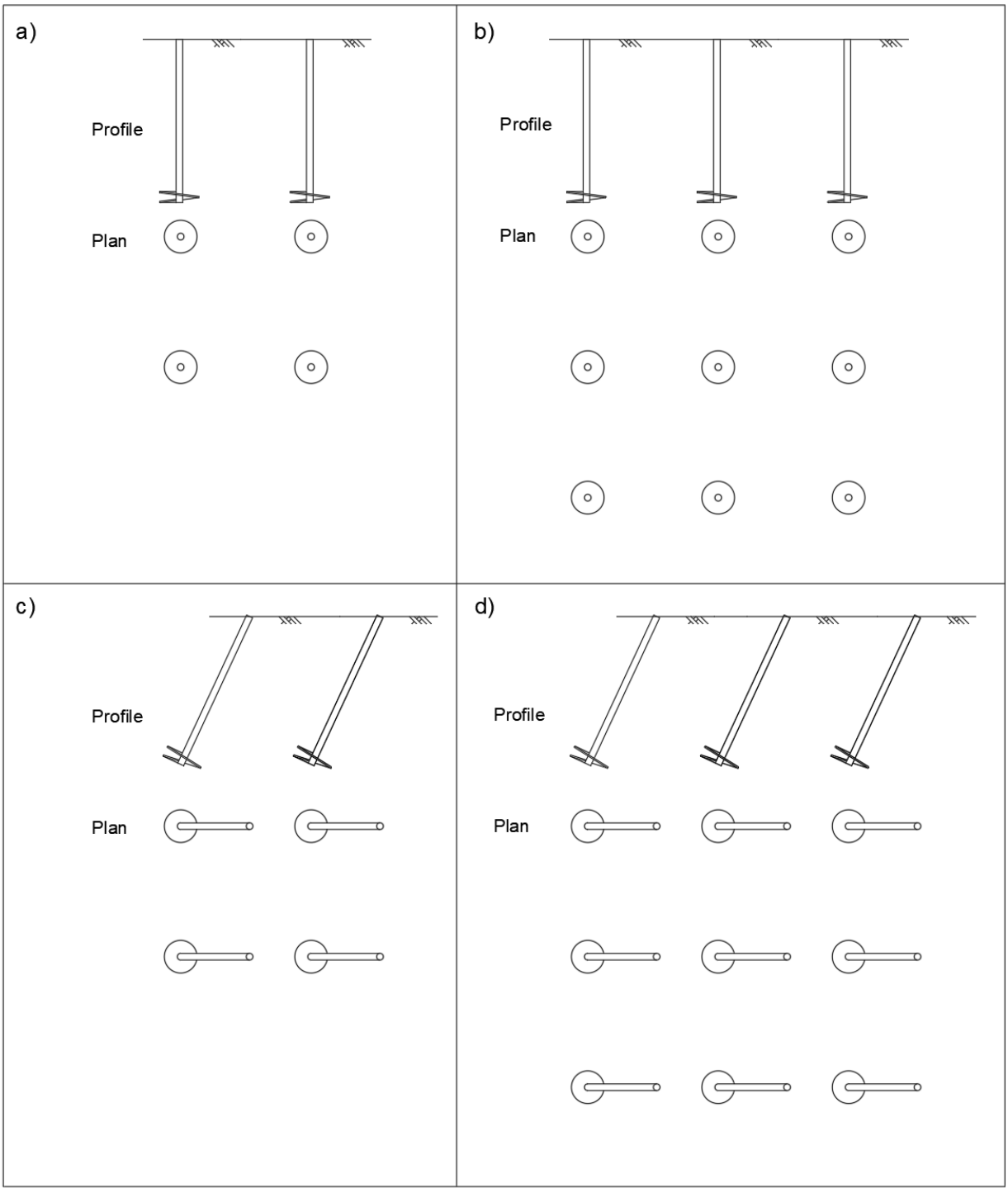

Figure 3.4. Helical Pile Groups Profile and Plan View: a) 2x2 Vertical, b) 3x3 Vertical, c) 2x2 25° Batter, d) 3x3 25° Batter.

Note: To Scale

3.5 CPT Method for Estimation of Installation Torque

This section describes methods used to estimate installation torque requirements for the helical piles designed in Section 4.1 and 4.2. As discussed in Section 2.3, installation torque can be predicted using correlations made between helical pile installation torque and CPT cone resistance data. Davidson et al. (2018) developed a method using a CPT profile for dense sand. The method from Davidson et al. (2018) and a synthetic CPT profile for the medium dense sand were used to predict installation torque. The following equations were used (Davidson et al. 2019).

(16) $T = T_s + T_b + \sum_1^n T_{h(n)}$

(17) $T_h = T_{h1} + T_{h2} + T_{h3}$

(18) $T_s = \sum_{\Delta x=1}^{\Delta xi=1} a\bar{q}_c tan\delta_{crit} \pi \Delta x \frac{D_s^2}{2}$

(19) $T_b = \bar{q}_c tan\delta_{crit} \pi \frac{D_s^3}{12}$

(20) $T_{h1} = a\bar{q}_c tan\delta_{crit} \pi \frac{D_h^2 - D_s^2}{12k_0}$

(21) $T_{h2} = a\bar{q}_c \tan(\delta_{crit} + \theta) \pi t \frac{D_h^2}{2}$

(22) $T_{h3} = a\bar{q}_c t \frac{D_h^2 - D_s^2}{4}$

(23) $a = \frac{F_r}{tan\delta_{crit}}$

(24) $k_0 = 1 - sin\varphi_{crit}$

(25) $\theta = tan^{-1}(\frac{p}{\pi} \frac{D_h - D_s}{2})$

where T is the total torque resulting during installation, T_s is the torque from the pile shaft area with diameter D_s, T_b is the torque from the base of the pile shaft, and T_h is the torque from the helical plate, with the diameter D_h, pitch of p, and plate thickness of t. A schematic of T_s, Tb, and Th locations is shown in Figure 3.5. T_h is composed of three components: T_{h1} is the friction on the underside of the helical plate during penetration, T_{h2} is the friction from the outside edge of the helical plate, and T_{h3} is the friction from the leading edge of the helical plate cutting into the soil. T_s is calculated as the sum of the intervals of length Δx over the total length of the pile shaft, L. a is the stress drop index, which is a function of the CPT friction ratio, F_r, which was generated from the CPT profile ranging linearly from 0.8% to 0.3% from the ground surface to 40 m depth. a is used to calculate the radial stress acting on the screw pile. The pitch angle, θ, is used to account for the inclination of the helical plate. δ_{crit} is the interface friction angle. k_0 is earth pressure at rest, which converts the radial stress, aq_c, into a vertical stress acting on the underside of the helix during installation. In this torque prediction method, influence from temperature was disregarded (Davidson et al. 2018).

The specific method of installation is ignored, as feasibility of installation is evaluated as the amount of torque required to install the helical pile.

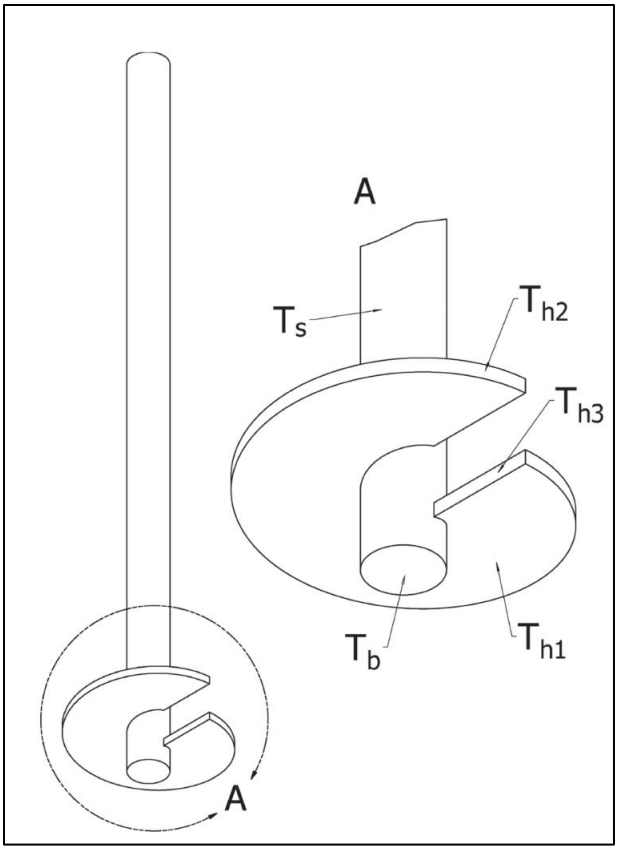

Figure 3.5. Installation Torques Acting on a Helical Pile (Davidson et al. 2018).

CHAPTER 4: PRESENTATION AND INTERPRETATION OF RESULTS

This chapter presents and analyzes results from single pile design, group pile design and installation torque estimations. This includes the design geometry and the lateral and axial capacities of single vertical piles and 2x2 and 3x3 vertical and battered groups installed in medium-dense sand and soft clay, radially battered helical pile groups and the estimated required installation torque for all pile sizes in sands.

Key assumptions made in this analysis are as follows:

1. In the soil profiles, strength linearly increases with depth
2. No thixotropic behavior is assumed for both the medium dense sand and the soft clay
3. Helical piles are designed with the same geometric proportions, i.e., Tables 3.6 and 3.7
4. Helical piles in groups are spaced a distance 4 times the helical plate diameter with the assumption that group efficiency is 100%
5. The method of connection between the mooring line and the helical pile group is not considered
6. The installation process is not considered, i.e., perfect installation, or 'wished in place' conditions are assumed
7. Maximum allowable mooring forces are adjusted with a Factor of Safety of 2

4.1 Single Helical Pile Design

This section presents and evaluates the design results for a vertical single helical pile installed in sand and clay. For the vertically installed helical piles, the maximum allowable anchor force from the mooring line is equivalent to the lateral capacity of the helical pile. The helical pile geometries, specified in Section 3.3.1, were solved for using the maximum anchor force and the

API method described in Section 3.3.2 for sand and clay for each of the four load cases: semisubmersible platform with multiline mooring system (SS-M), semisubmersible platform with single line mooring system (SS-S), spar buoy platform with multiline mooring system (SB-M) and spar buoy platform with single line mooring system (SB-S).

The axial capacities were calculated using methods described in Section 3.3.3. The results for the four load cases in the dense sand and soft clay are presented in Table 4.1 and 4.2 respectively. In sand, as expected, the SS-S case with the largest maximum anchor force, resulted in the largest size pile with a required length of 13.4 meters and helix diameter of 2.68 meters. The smallest maximum anchor force, from the SB-M case, resulted in the smallest pile with a length of 9.2 meters and a helix diameter of 1.84 meters. In the soft clay, the helical piles needed to be larger to meet the required capacity to resist the same maximum anchor forces. In clay, the SS-S case also had the largest pile design out of the four load cases, with a pile length of 25.1 meters and a helix diameter of 5.01 meters. The SB-M case also had the smallest pile design in clay, with a length of 17.0 meters and helix diameter of 3.4 but is larger than any single piles designed for sand.

Figure 4.1 presents the helical pile shaft length designed for each load case in sand and clay, and shows that the soft clay requires a larger pile than in dense sand for the same load case. This figure also shows the magnitude of anchor forces for each load case directly influences pile geometry. The anchor forces for the semisubmersible platform are larger than the that for the spar buoy, which is constant with the pile length presented within soil type. Multiline mooring systems have a smaller anchor force than single line mooring systems, which is reflected in the figure for each platform type.

Table 4.1. Design Results for Four Load Cases for Single Round-Shaft, Vertically Installed, Single Helix Helical Pile – Sand.

Pile Dimensions (m)					
Platform and Mooring Type		Semi Submersible		Spar Buoy	
		Multi-Line	Single-Line	Multi-Line	Single-Line
Shaft Length	L	13.4	14.2	9.2	11.8
Shaft Diameter	D_S	0.54	0.57	0.37	0.47
Helix Diameter	D_H	2.68	2.84	1.84	2.35
Helix Pitch	p	0.80	0.85	0.55	0.71
Helix Thickness	t_H	0.11	0.11	0.07	0.09
Shaft Thickness	t_S	0.012	0.012	0.010	0.011
Weight (kg)	W	6819	8042	2366	4700
Pile Capacity (kN)					
Platform Type		Semi Submersible		Spar Buoy	
Mooring Setup		Multi-Line	Single-Line	Multi-Line	Single-Line
Allowable Force		4302	5120	1368	2888
Lateral Capacity		4320	5141	1398	2913
Uplift Capacity		30889	36758	9997	20826
Compressive Capacity		31195	37123	10096	21032

Table 4.2. Design Results for Four Load Cases for Single Round-Shaft, Vertically Installed, Single Helix Helical Pile – Clay.

Pile Dimensions (m)					
Platform and Mooring Type		Semi Submersible		Spar Buoy	
		Multi-Line	Single-Line	Multi-Line	Single-Line
Shaft Length	L	25.1	26.6	17.0	21.9
Shaft Diameter	D_S	1.00	1.06	0.68	0.88
Helix Diameter	D_H	5.01	5.31	3.4	4.38
Helix Pitch	p	1.50	1.59	1.02	1.31
Helix Thickness	t_H	0.20	0.21	0.14	0.18
Shaft Thickness	t_S	0.016	0.017	0.013	0.015
Weight (kg)	W	41241	48844	13455	27925
Pile Capacity (kN)					
Platform Type		Semi Submersible		Spar Buoy	
Mooring Setup		Multi-Line	Single-Line	Multi-Line	Single-Line
Allowable Force		4302	5120	1368	2888
Lateral Capacity		4321	5135	1373	2902
Uplift Capacity		5581	6586	1899	3819
Compressive Capacity		6692	7908	2247	4562

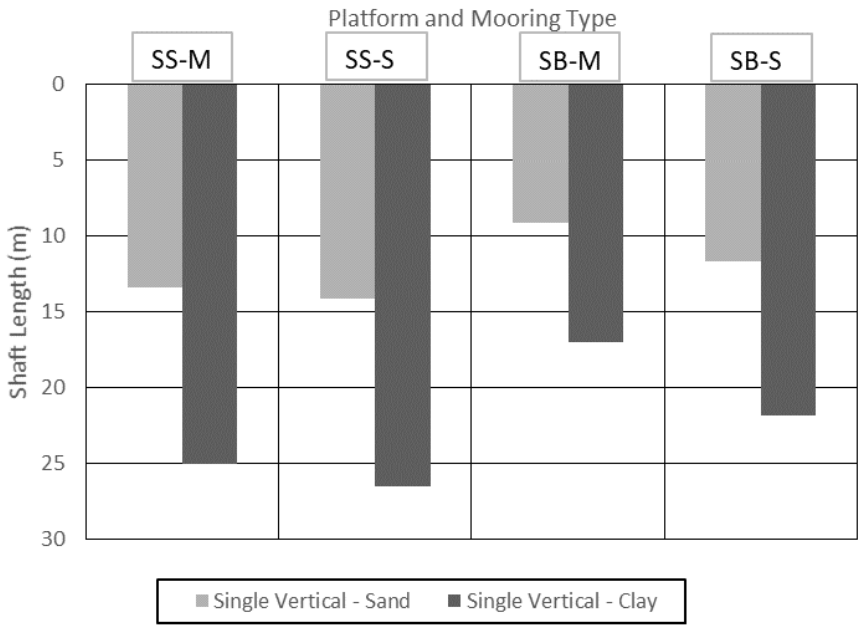

Figure 4.1. Shaft Length for Single Helical Piles in Sand and Clay.

From Table 4.1 and 4.2, the lateral capacities for both soil types are much smaller in comparison to the axial capacities: uplift and compressive capacity. The lateral capacity is smaller firstly because the method for calculating the lateral capacity assumes the influence of the helix is negligible, and secondly because lateral capacity depends primarily on shaft diameter, which are small for helical piles to reduce the required installation torque. The axial capacities, however, do account for the helix. The compressive capacity is slightly larger than the uplift, which agrees with Terzaghi's equations, where in compressive conditions the bearing area is the net area of the helical plate and the base of the shaft. In uplift conditions, the bearing area is just the net area of the helical plate. The contribution from shaft resistance is the same for uplift and compressive capacity calculations for the same size pile. As expected, the helical anchor is not an effective foundation for lateral loading compared to axial loading.

Figure 4.2 compares the lateral, uplift and compressive capacities of helical piles for each load case in both soils. The lateral capacities between each soil type for each load case are nearly the same because they were set as the limiting capacity. For clays, the axial capacities are clearly

larger than the lateral, but only slightly when compared to the axial capacities from the piles in sand. The dense sand provides more resistance to the pile than the soft clay, which increases the pile capacity and decreases the required pile size to resist the same load. Even though the pile designed for sand is smaller than the pile designed for clay, it still has much larger axial capacities. To take advantage of this large axial capacity in strictly horizontal loading conditions, the helical pile can be installed at a batter which is investigated in Section 4.2.

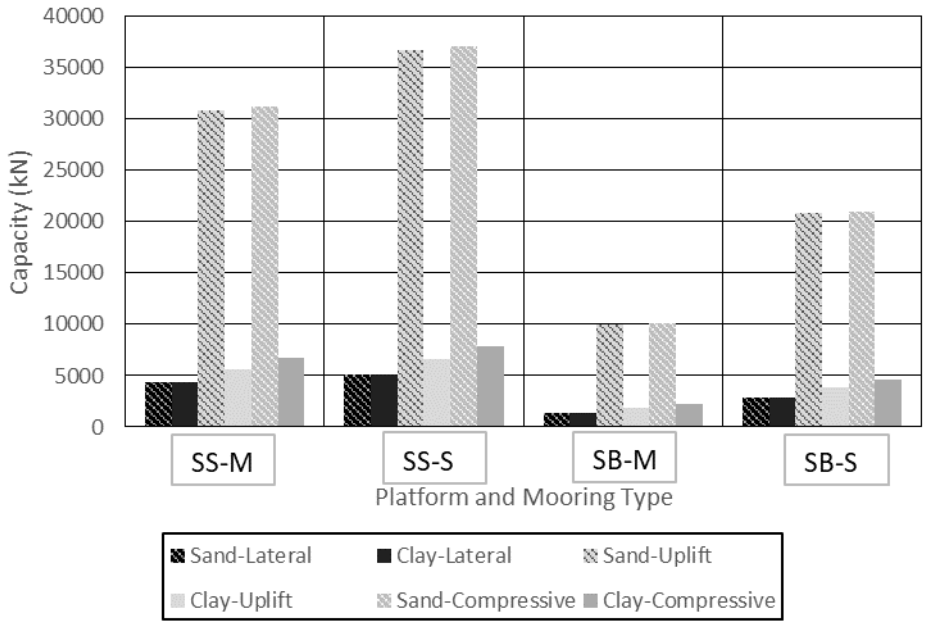

Figure 4.2. Capacities for Single Helical Piles in Sand and Clay (note: for these data the lateral capacity is the required design force; hence the values are the same for sand and clay but the pile dimensions are different).

The weight of the helical piles was calculated using a density of steel equal to 7,900 kg/m^3. Figure 4.3 illustrates the weight of the helical piles for the four load cases and two soil types. The weight is proportional to the mooring force, where the semisubmersible platform load cases require a larger pile compared to the spar buoy cases. Likewise, the piles installed in clay are much heavier than those needed for sand.

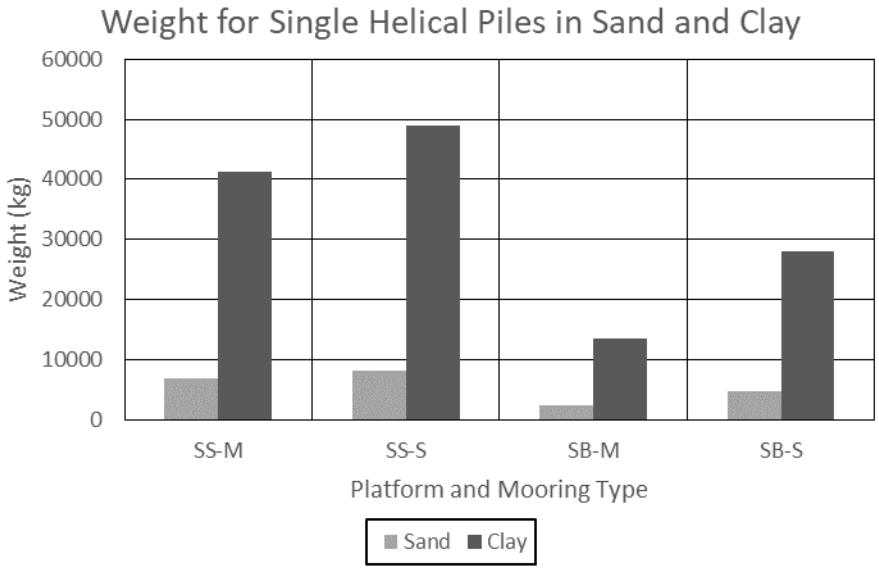

Figure 4.3. Weight of steel for Single Helical Piles in Sand and Clay.

To compare how shaft length influences lateral capacity, Table 4.3 presents the geometry, lateral capacity, weight and efficiency for four helical piles designed in soft clay soil. The first helical pile was designed for semisubmersible single line loading conditions from Table 4.2. The three other piles are designed with the same recommended size proportions (i.e., Table 3.6) but decrease in shaft length by 5 meters increments. Figure 4.4, which plots a) lateral capacity and b) weight as a function of shaft length, illustrates how shaft length changes lateral capacity and weight as a power relationship. The power relationship in a) comes from the API equations used to find lateral capacity and the power relationship in b) is from the equations used to calculate the weight of the pile.

Table 4.3. Geometry (m), Lateral Capacity (kN) and Weight (kg) for a Helical Pile in Soft Clay.

Shaft Length (m)	L	26.6	25	20	15
Shaft Diameter (m)	D_S	1.06	1.00	0.80	0.60
Helix Diameter (m)	D_H	5.31	5.00	4.00	3.00
Helix Pitch (m)	p	1.59	1.50	1.20	0.90
Helix Thickness (m)	t_H	0.21	0.20	0.16	0.12
Shaft Thickness (m)	t_S	0.017	0.016	0.014	0.012
Lateral Capacity (kN)	Q_{lat}	5135	4296	2219	950
Weight (kg)	W	48844	41002	21480	9403
Efficiency	Q_{lat}/W	0.1051	0.1048	0.1033	0.1010

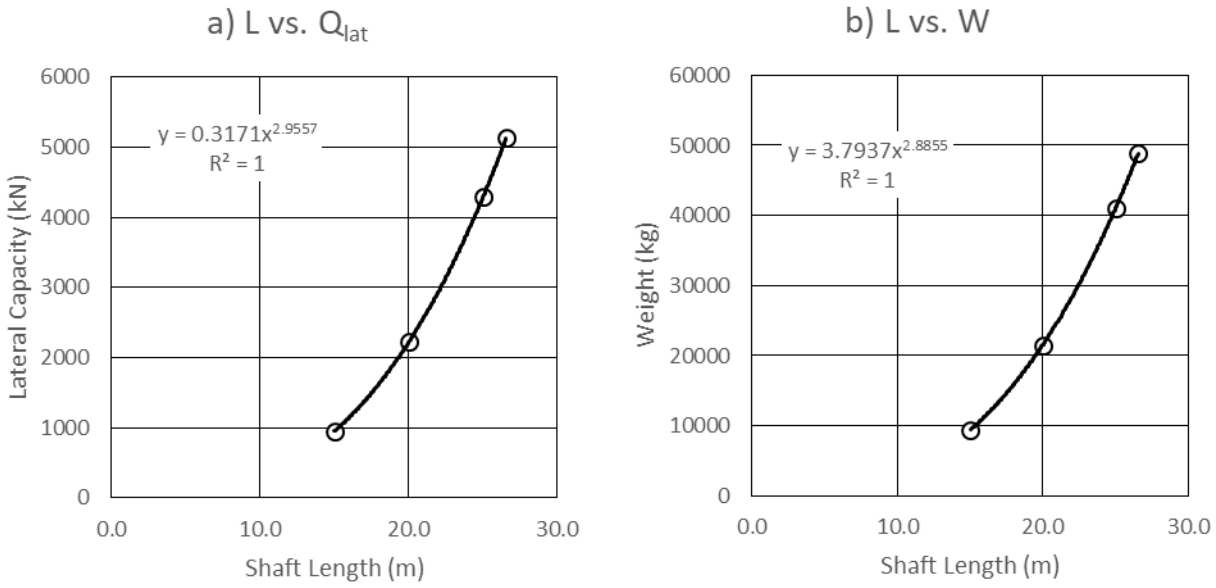

Figure 4.4. a) Shaft Length vs. lateral Capacity, b) Shaft Length versus Weight for Helical Piles in Soft Clay.

Helical piles are compared to suction caissons, a method of anchoring already used for design of floating offshore structures (e.g., Equinor's Hywind project offshore Scotland). This comparison evaluates the efficiency of helical piles versus suction caissons in terms of capacity per unit weight. Table 4.4 and Table 4.5 present the design results for a single vertically installed steel suction caisson for each load case in medium dense sand and clay respectively, using the $L/D_S = 3$ and wall thickness of $t = D_S/144$.

Figure 4.5 compares the weight of helical piles and suction caissons in both soil types for each of the four load cases. Isolating by soil type, helical piles have lower weight of steel than suction caissons in every load case, decreasing the amount and cost of materials needed. A significant part of the difference is that the thickness of the suction caissons is greater than that of the helical pile shafts. The maximum anchor force, or required lateral capacity for these vertical piles, is normalized by the weight of the anchor to compare the anchor efficiency. The normalized capacities for helical piles are presented in Table 4.6, and for suction caissons in Table 4.7. Figure 4.6 plots the normalized capacities for both anchor types. In this figure it is clear that the helical piles, for both sand and clay, are more efficient than suction caissons, having more capacity per unit of weight.

Table 4.4. Design Results for Single Suction Caissons, Vertically Installed in Sand.

Suction Caisson Dimensions (m)					
Platform and Mooring Type		Semi Submersible		Spar Buoy	
		Multi-Line	Single-Line	Multi-Line	Single-Line
Single Pile	L	7.93	8.40	5.41	6.94
	D	2.64	2.80	1.80	2.31
	t	0.018	0.019	0.013	0.016
	W (kg)	9476	11260	3017	6357

Table 4.5. Design Results for Single Suction Caissons, Vertically Installed in Clay.

Suction Caisson Dimensions (m)					
Platform and Mooring Type		Semi Submersible		Spar Buoy	
		Multi-Line	Single-Line	Multi-Line	Single-Line
Single Pile	L	14.77	15.67	10.03	12.91
	D	4.92	5.22	3.34	4.30
	t	0.034	0.036	0.023	0.030
	W (kg)	61321	73127	19177	40903

Table 4.6. Normalized Capacity for Single Helical Piles in Sand and Clay.

Normalized Capacity - Qlateral/W (kN/kg)				
Platform Type	Single-Line		Single-Line	
Mooring Setup	Multi-Line	Single-Line	Multi-Line	Single-Line
Clay	0.10	0.11	0.10	0.10
Sand	0.63	0.64	0.59	0.62

Table 4.7. Normalized Capacity for Single Suction Caissons in Sand and Clay

Normalized Capacity - $Q_{lateral}$/W (kN/kg)				
Platform Type	Single-Line		Single-Line	
Mooring Setup	Multi-Line	Single-Line	Multi-Line	Single-Line
Clay	0.07	0.07	0.07	0.07
Sand	0.45	0.45	0.45	0.45

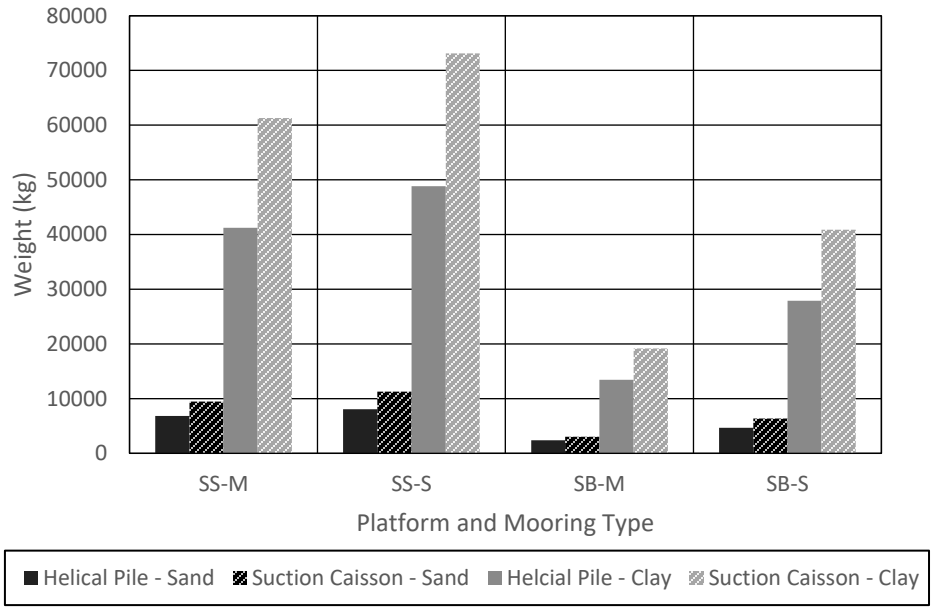

Figure 4.5. Weight for Single Helical Piles and Suction Caissons in Sand and Clay.

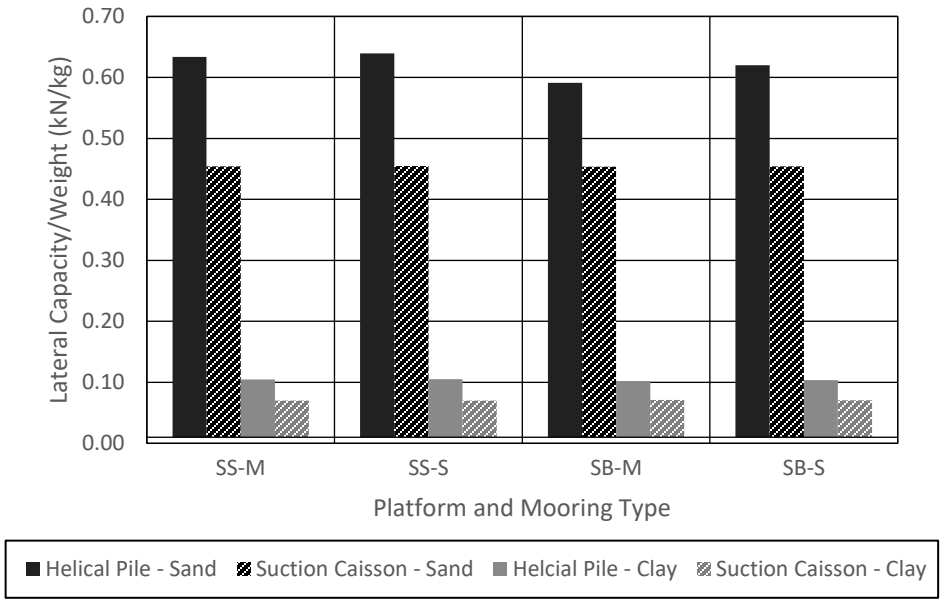

Figure 4.6. Normalized Capacity for Single Helical Piles and Suction Caissons in Sand and Clay.

4.2 Helical Pile Group Design

This section presents and evaluates the results from group pile designs installed in sand and clay. Like for the single vertical helical piles, the maximum anchor force from the mooring line is equivalent to the lateral capacity of the helical pile group. For each group, the group efficiency is assumed to be 1 to evenly distribute the maximum anchor force. For each pile in helical pile groups in a 2x2 square layout, the maximum anchor force was distributed evenly among the 4 helical piles, so the desired lateral capacity is equal to 1/4 the maximum anchor force. For each pile in battered helical pile groups in a 2x2 square layout, the maximum anchor force was distributed evenly among the 4 helical piles, so the desired lateral capacity is equal to 1/4 the maximum anchor force times the cosine of the 25 degree batter. For each pile in helical pile groups in a 3x3 square layout, the maximum anchor force was distributed evenly among the 9 helical piles, so the desired lateral capacity is equal to 1/9 the maximum anchor force. For each pile in battered helical pile groups in a 3x3 square layout, the maximum anchor force was distributed

evenly among the 9 helical piles, so the desired lateral capacity is equal to 1/9 the maximum anchor force times the cosine of the 25 degree batter.

Table 4.8 presents the required lateral capacity component of the maximum anchor force for individual battered piles. The helical pile geometries were solved for using the same API methods used for single piles and the same four load conditions: SS-M, SS-S, SB-M and SB-S.

Table 4.8. Required Lateral Component for Individual Piles in Pile Groups with a Batter of 25°.

Required Lateral Component with Batter				
Platform and Mooring Type	Semi Submersible		Spar Buoy	
	Multi-Line	Single-Line	Multi-Line	Single-Line
Allowable Force	2151	2560	684	1444
FS = 2	4302	5120	1368	2888
Lateral Component with a 25 Degree Batter (kN)	Single Pile			
	3899	4640	1240	2617
	1 Pile in 2x2 Group			
	975	1160	310	654
	1 Pile in 3x3 Group			
	433	516	138	291

The axial capacities were then calculated per pile using methods described in Section 3.3.3. The geometry and capacity results of the four pile groups for each load cases in sand are presented in Table 4.9 and Table 4.10 respectively with the results from single piles in Section 4.1 for comparison. The corresponding results in clay are presented in Table 4.11 and 4.12. Similar trends in the design results for single piles are seen with the pile groups, where in both sand and clay, the SS-S case with the largest maximum anchor force resulted with the largest pile geometry. The smallest maximum anchor force from the SB-M case resulted with the smallest pile design for each group. Like for single piles, the soft clay soil requires larger helical piles to meet the required capacity needed to resist the same maximum anchor forces in sand. Overall, the vertical piles

needed in pile groups are significantly smaller than the single vertical piles. The battered piles in both soil types are slightly smaller than the vertical piles in the same group size; this is expected as the use of axial capacity in battered piles reduces the length of the pile needed for resisting only with lateral capacity.

Table 4.9. Design Results for Four Load Cases for Pile Group Single, 2x2 and 3x3 Load, Round-Shaft, Vertical and 25° Batter, Single Helix Helical Pile – Sand.

Pile Dimensions [m]			Shaft Length	Shaft Diameter	Helix Diameter	Helix Pitch	Helix Thickness	Shaft Thickness	Weight (kg)
Pile Type	Platform Type	Mooring Type	L	D_S	D_H	p	t_H	t_S	W
Single Vertical	Semisubmersible	Multi-Line	13.4	0.54	2.68	0.80	0.11	0.012	6819
		Single-Line	14.2	0.57	2.84	0.85	0.11	0.012	8042
	Spar Buoy	Multi-Line	9.2	0.37	1.84	0.55	0.07	0.010	2366
		Single-Line	11.8	0.47	2.35	0.71	0.09	0.011	4700
Group 1/4	Semisubmersible	Multi-Line	8.5	0.34	1.69	0.51	0.07	0.010	1868
		Single-Line	9.0	0.36	1.79	0.54	0.07	0.010	2191
	Spar Buoy	Multi-Line	5.8	0.23	1.16	0.35	0.05	0.009	666
		Single-Line	7.4	0.30	1.48	0.44	0.06	0.009	1295
Group 1/4 Battered 25	Semisubmersible	Multi-Line	8.2	0.33	1.64	0.49	0.07	0.010	1719
		Single-Line	8.7	0.35	1.73	0.52	0.07	0.010	1993
	Spar Buoy	Multi-Line	5.6	0.22	1.12	0.34	0.04	0.009	606
		Single-Line	7.2	0.29	1.43	0.43	0.06	0.009	1178
Group 1/9 Vertical	Semisubmersible	Multi-Line	6.5	0.26	1.29	0.39	0.05	0.009	900
		Single-Line	6.9	0.27	1.37	0.41	0.05	0.009	1048
	Spar Buoy	Multi-Line	4.4	0.18	0.88	0.26	0.04	0.008	318
		Single-Line	5.7	0.23	1.13	0.34	0.05	0.009	621
Group 1/9 Battered 25	Semisubmersible	Multi-Line	6.2	0.25	1.24	0.37	0.05	0.009	798
		Single-Line	6.6	0.26	1.32	0.40	0.05	0.009	946
	Spar Buoy	Multi-Line	4.3	0.17	0.85	0.26	0.03	0.008	290
		Single-Line	5.5	0.22	1.10	0.33	0.04	0.009	577

Table 4.10. Capacity Results for Four Load Cases for Pile Group Single, 2x2 and 3x3 Load, Round-Shaft, Vertical and 25° Batter, Single Helix Helical Pile – Sand.

Pile Capacity [kN]			Total Allowable Force	Allowable Force Per Pile	Allowable Lateral Force	Allowable Uplift Force	Lateral Capacity	Uplift Capacity	Compressive Capacity
Pile Type	Platform Type	Mooring Type							
Single Vertical	Semisubmersible	Multi-Line	4302	-	4302	-	4320	30889	31195
		Single-Line	5120	-	5120	-	5141	36758	37123
	Spar Buoy	Multi-Line	1368	-	1368	-	1398	9997	10096
		Single-Line	2888	-	2888	-	2913	20826	21032
Group 1/4	Semisubmersible	Multi-Line	4302	1076	1076	-	1083	7746	7822
		Single-Line	5120	1280	1280	-	1287	9204	9295
	Spar Buoy	Multi-Line	1368	342	342	-	350	2505	2530
		Single-Line	2888	722	722	-	728	5202	5254
Group 1/4 Battered 25	Semisubmersible	Multi-Line	4302	1076	975	455	990	6415	6479
		Single-Line	5120	1280	1160	541	1162	7530	7605
	Spar Buoy	Multi-Line	1368	342	310	145	315	2043	2064
		Single-Line	2888	722	654	305	656	4253	4295
Group 1/9 Vertical	Semisubmersible	Multi-Line	4302	478	478	-	482	3445	3479
		Single-Line	5120	569	569	-	577	4126	4167
	Spar Buoy	Multi-Line	1368	152	152	-	153	1094	1104
		Single-Line	2888	321	321	-	324	2315	2338
Group 1/9 Battered 25	Semisubmersible	Multi-Line	4302	478	433	202	438	2163	2185
		Single-Line	5120	569	516	240	516	2610	2636
	Spar Buoy	Multi-Line	1368	152	138	64	138	697	704
		Single-Line	2888	321	291	136	299	1510	1525

Table 4.11. Design Results for Four Load Cases for Pile Group Single, 2x2 and 3x3 Load, Round-Shaft, Vertical and 25° Batter, Single Helix Helical Pile – Clay.

Pile Dimensions [m]			Shaft Length	Shaft Diameter	Helix Diameter	Helix Pitch	Helix Thickness	Shaft Thickness	Weight per Pile (kg)
Pile Type	Platform Type	Mooring Type	L	D_S	D_H	p	t_H	t_S	W
Single Vertical	Semisubmersible	Multi-Line	25.1	1.00	5.01	1.50	0.20	0.016	41241
		Single-Line	26.6	1.06	5.31	1.59	0.21	0.017	48844
	Spar Buoy	Multi-Line	17.0	0.68	3.40	1.02	0.14	0.013	13455
		Single-Line	21.9	0.88	4.38	1.31	0.18	0.015	27925
Group 1/4	Semisubmersible	Multi-Line	15.7	0.63	3.13	0.94	0.13	0.013	10615
		Single-Line	16.6	0.66	3.32	1.00	0.13	0.013	12566
	Spar Buoy	Multi-Line	10.6	0.42	2.12	0.64	0.08	0.011	3517
		Single-Line	13.7	0.55	2.74	0.82	0.11	0.012	7262
Group 1/4 Battered 25	Semisubmersible	Multi-Line	15.2	0.61	3.04	0.91	0.12	0.012	9765
		Single-Line	16.2	0.65	3.23	0.97	0.13	0.013	11615
	Spar Buoy	Multi-Line	10.3	0.41	2.06	0.62	0.08	0.010	3244
		Single-Line	13.3	0.53	2.66	0.80	0.11	0.012	6676
Group 1/9 Vertical	Semisubmersible	Multi-Line	11.9	0.48	2.38	0.71	0.10	0.012	4946
		Single-Line	12.6	0.50	2.52	0.76	0.10	0.011	5726
	Spar Buoy	Multi-Line	8.1	0.32	1.61	0.48	0.06	0.010	1633
		Single-Line	10.4	0.42	2.08	0.62	0.08	0.011	3333
Group 1/9 Battered 25	Semisubmersible	Multi-Line	11.6	0.46	2.31	0.69	0.09	0.011	4478
		Single-Line	12.3	0.49	2.45	0.74	0.10	0.011	5287
	Spar Buoy	Multi-Line	7.8	0.31	1.56	0.47	0.06	0.009	1497
		Single-Line	10.1	0.40	2.01	0.60	0.08	0.010	3028

Table 4.12. Capacity Results for Four Load Cases for Pile Group Single, 2x2 and 3x3 Load, Round-Shaft, Vertical and 25° Batter, Single Helix Helical Pile – Clay.

Pile Capacity [kN]			Total Allowable Force	Allowable Force Per Pile	Allowable Lateral Force	Allowable Uplift Force	Lateral Capacity	Uplift Capacity	Compressive Capacity
Pile Type	Platform Type	Mooring Type							
Single Vertical	Semisubmersible	Multi-Line	4302	-	4302	-	4321	5581	6692
		Single-Line	5120	-	5120	-	5135	6586	7908
	Spar Buoy	Multi-Line	1368	-	1368	-	1373	1899	2247
		Single-Line	2888	-	2888	-	2902	3819	4562
Group 1/4	Semisubmersible	Multi-Line	4302	1076	1076	-	1076	1520	1792
		Single-Line	5120	1280	1280	-	1280	1781	2105
	Spar Buoy	Multi-Line	1368	342	342	-	343	561	646
		Single-Line	2888	722	722	-	727	1071	1253
Group 1/4 Battered 25	Semisubmersible	Multi-Line	4302	1076	975	455	979	1312	1392
		Single-Line	5120	1280	1160	541	1171	1547	1639
	Spar Buoy	Multi-Line	1368	342	310	145	313	477	512
		Single-Line	2888	722	654	305	661	917	978
Group 1/9 Vertical	Semisubmersible	Multi-Line	4302	478	478	-	481	747	866
		Single-Line	5120	569	569	-	569	863	1005
	Spar Buoy	Multi-Line	1368	152	152	-	154	296	333
		Single-Line	2888	321	321	-	325	536	616
Group 1/9 Battered 25	Semisubmersible	Multi-Line	4302	478	433	202	437	636	681
		Single-Line	5120	569	516	240	520	740	791
	Spar Buoy	Multi-Line	1368	152	138	64	139	247	268
		Single-Line	2888	321	291	136	291	449	483

Table 4.13 shows the percent decrease in shaft length of battered helical piles compared to vertical helical piles for both soil types and group sizes. Overall, there is about a 3.3% decrease in shaft length for battered helical piles in sand, and 2.9% in clay. Since all helical piles have proportional dimensions, this also implies a 3.3% and 2.9% decrease in overall size for helical piles in sand and clay respectively with a 25° batter.

Table 4.13 Percent Decrease in Battered Helical Pile Shaft Length.

Platform Type		Semi Submersible		Spar Buoy	
Mooring Setup		Multi-Line	Single-Line	Multi-Line	Single-Line
Sand	2x2	3.0	3.4	3.4	3.4
	3x3	3.9	3.6	3.4	2.7
Clay	2x2	2.9	2.7	2.8	2.9
	3x3	2.9	2.8	3.1	3.4

Figure 4.7 presents the helical pile shaft length for single piles and pile groups designed for each load case in sand and clay soil. The figure clearly shows that soft clay requires a larger pile than the sand, and that the increasing group size, and adding a batter, decreases the required pile length. It is noticeable that the pile length does not decrease proportionally to the required lateral capacity; the piles in the group of 2x2 are not one quarter the length of the single pile and the piles in the group of 3x3 are not one ninth the length of the single pile.

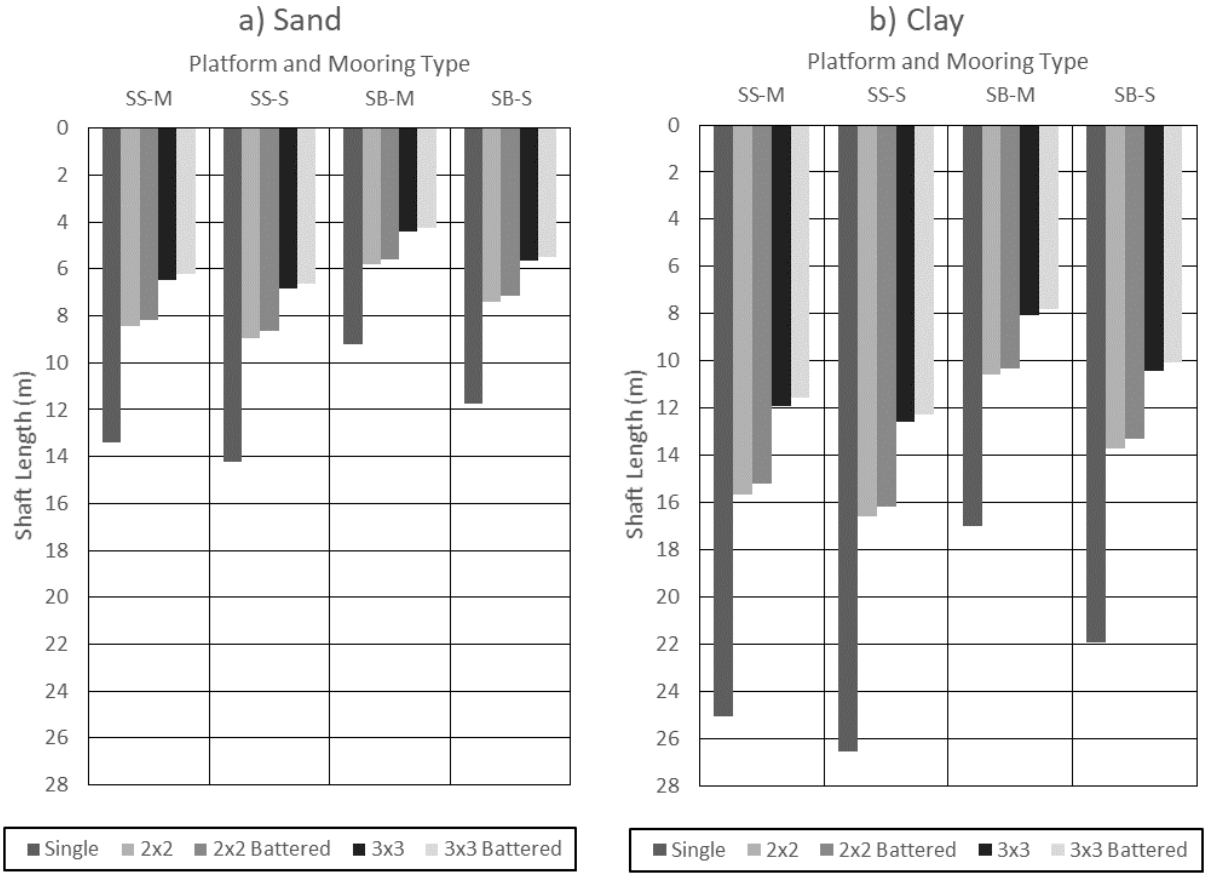

Figure 4.7. Shaft Length for Helical Piles in a) Sand, b) Clay.

This relationship of lateral capacity and shaft length is plotted in Figure 4.8 for vertical piles. For both soil types, the relationship between lateral capacity and shaft length is not linear, rather a function of the resistance – deflection equations used in the API method. The difference

between the data trends for sand and clay can be attributed to the soil properties, particularly the strength gradient, where the sand is stronger and therefore offers more resistance with depth than the clay. More resistant soil correlates to a smaller pile design.

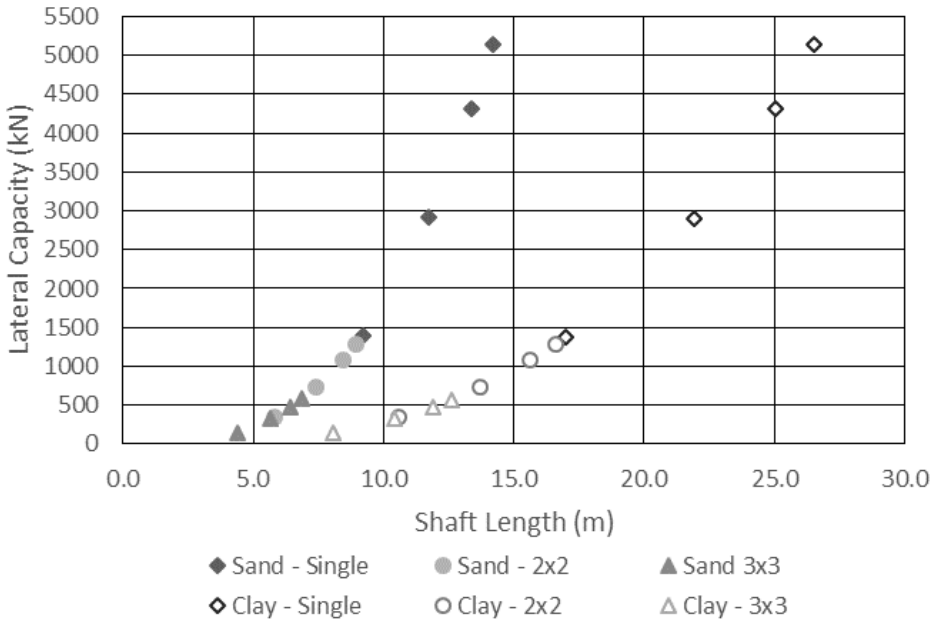

Figure 4.8. Lateral Capacity versus Shaft Length for Vertical Helical Piles.

The weight of the helical pile groups and single piles is compared to determine which uses less material under the same load. The weight of the helical pile groups was determined using the same method for single piles, where the volume of a single pile in the group was found using the design dimensions and then multiplied by the number of piles, either 4 or 9, to determine the net weight of the group. Figure 7.9 illustrates the net weight of the helical pile groups and compares to the weight of single piles and suction caissons designed for the same load cases. The net weights of both 2x2 and 3x3 pile group sizes, vertical and battered, are larger than the weight of a single pile for each load case in sand. In clay, the battered pile groups' net weight is less than a single pile for each load case. In both soils, the net weights of single helical piles and helical pile groups are significantly less than suction caissons.

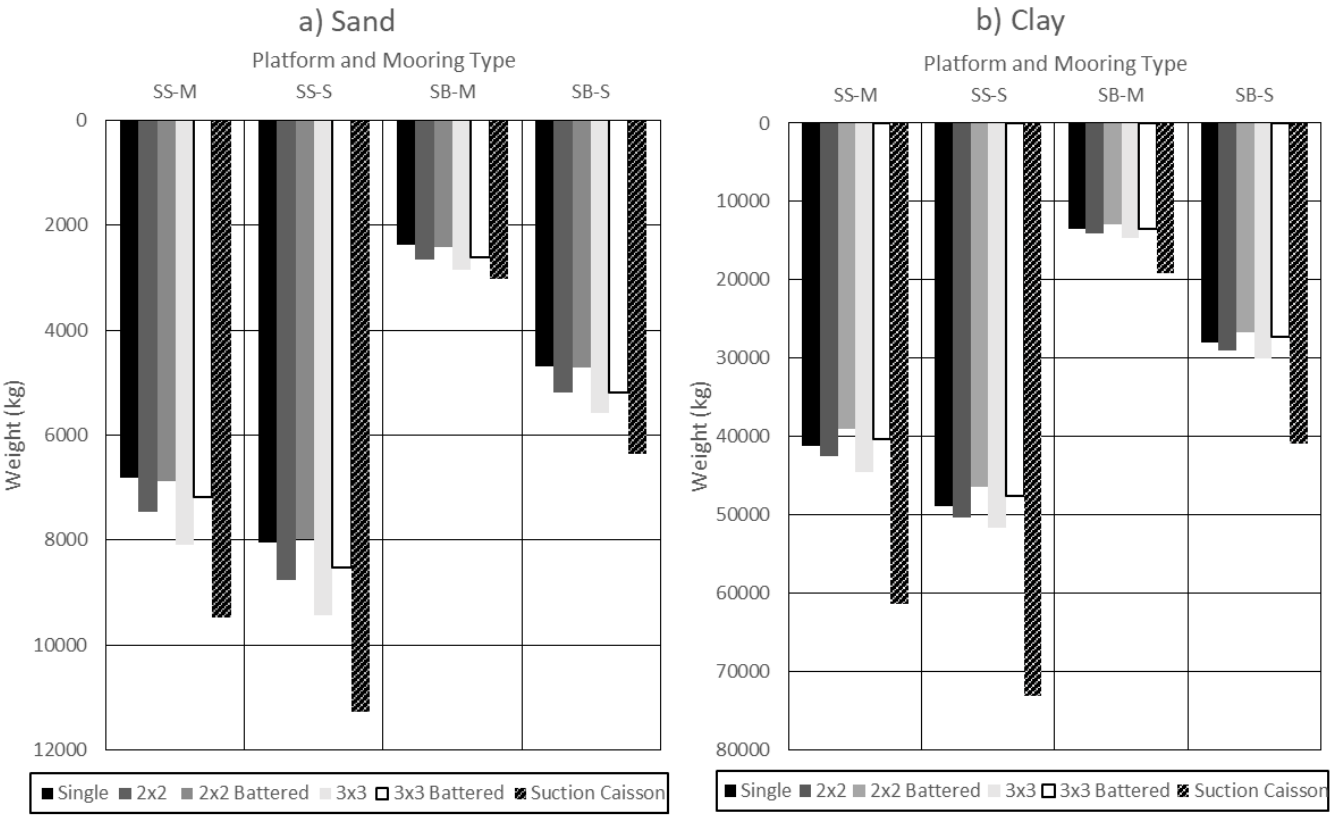

Figure 4.9. Net Weight for Helical Piles and Suction Caissons in a) Sand, b) Clay – Semi-Log Scale.

Even though the net weight of helical pile groups is larger than the equivalent single pile, the smaller geometries of the helical piles used in groups, particularly the shaft and helix diameters, will require less torque for installation. Results for required installation torque estimations is presented in Section 4.3.

4.3 Radially Battered Helical Pile Groups

For an FOWT multiline system, it is likely that the maximum mooring line force will not always be in the same direction but could rotate slightly in changing weather conditions. The following section discusses how changing the direction of the mooring force affects the capacity of a particular pile group and a potential design consideration for reducing loss of capacity. The

battered pile group arraigned in a 2x2 square and the design lateral and axial capacities previously calculated for a semisubmersible platform and multiline catenary mooring system are used (Table 4.14). For the calculations and figures in this section, it is assumed that the mooring force rotation angle is found between the mooring force direction and direction of pile batter.

Table 4.14. Capacities for a 25 Battered Helical Pile in a 2x2 Layout Under SS-M Loading Conditions.

Capacity	kN
Lateral	990
Uplift	6415
Compressive	6479

The original battering of the helical pile groups assumes that the maximum mooring force is in line with the pile shaft and oriented away from the helix. This is shown in Figure 4.10, where the mooring force direction is illustrated with an arrow. The capacity of an individual pile is calculated by taking the sum of the portion of the axial and lateral capacities acting in the same direction as the mooring line force. For an individual pile in Figure 4.10, the capacity is estimated using equation 26. Then, since the piles are all oriented the same way relative to the direction of the mooring force, the capacity of one pile is multiplied by the number of piles to find the capacity of the group, shown in equation 27. The capacity of the group is estimated to be 14,433 kN.

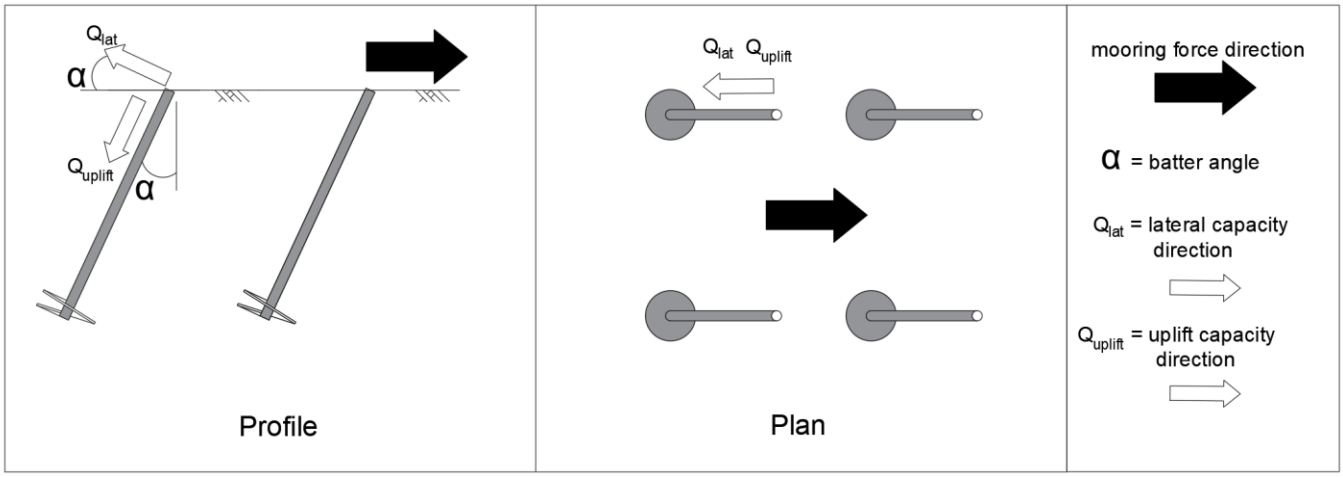

Figure 4.10. Uniformly Battered Pile Group with Mooring Force in Line with Batter Direction.

(26) $F_{pile} = Q_{lat}\cos(\alpha) + Q_{uplift}\sin(\alpha)$

(27) $F_{group} = \sum_{i=1}^{n} F_{pile}, i$

If the mooring force is not acting in the same direction as the battered piles, but instead acts at an angle between 0° and 90° from the direction of batter, as shown in Figure 4.11, the capacity of the group decreases. The capacity of an individual pile is then the sum of the loading direction components of the axial capacities acting in the direction of the batter and the reduced lateral capacity acting against the direction of batter, shown in equation 28.

(28) $F_{pile} = \left[Q_{uplift}\sin(\alpha)\right]\cos(\beta) + Q_{lat}\cos\left(\alpha \times \frac{90-\beta}{90}\right)$

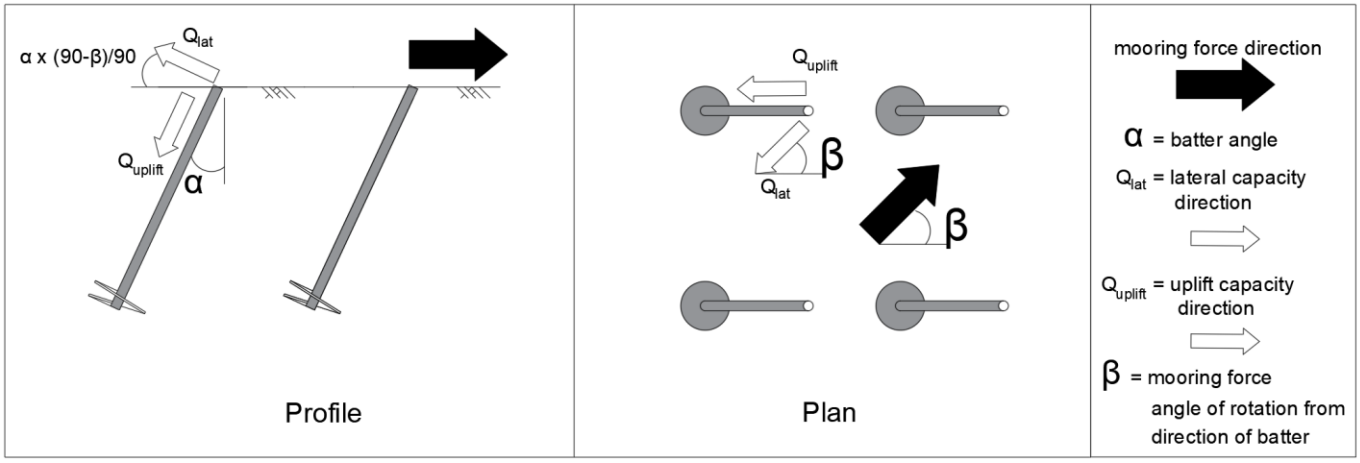

Figure 4.11. Uniformly Battered Pile Group with Mooring Force Angled from Batter Direction.

The capacity of the group can be estimated using equation 27. For Figure 4.11, if the rotation angle of the mooring force is 45 degrees from the batter direction, the capacity of the group is calculated to be 11,534 kN. Rotating the mooring force direction from Figure 4.10 to the direction in Figure 4.11 shows about a 20% decrease in capacity.

Figure 4.12 shows a scenario where the mooring force rotation angle is 90° from the direction of batter. In this case, only the lateral capacity of the pile is contributing to resistance against the mooring force. The individual pile capacity is equal to the lateral capacity, shown in equation 29. The capacity of the group can be found using equation 27. For Figure 4.12 the capacity of the group is estimated to be 3,960 kN, which is about a 73% decrease in capacity from Figure 4.10.

(29) $F_{pile} = Q_{lat}$

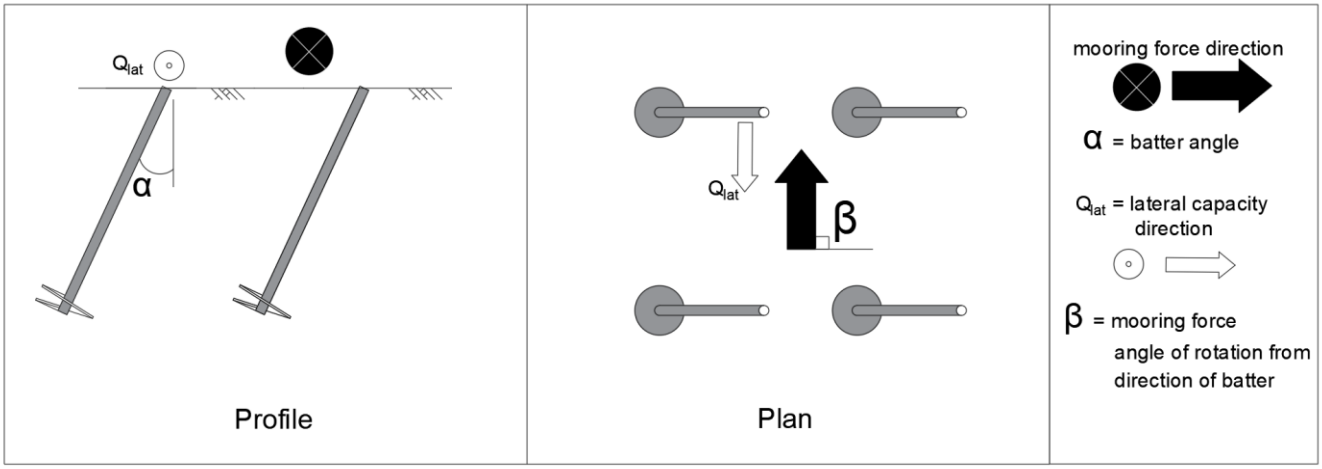

Figure 4.12. Uniformly Battered Pile Group with Mooring Force Perpendicular from Batter Direction.

One design consideration to reduce the loss in capacity with changing mooring force directions is to batter the helical piles radially. Radial battering the helical piles towards a central point increases the symmetry of the group and changes how the individual piles resist the mooring force. Figure 4.13 shows the 2x2 pile group with radial battering. The battering angle is still 25 degrees from vertical and pile spacing of $4D_h$ from the top of the pile shaft is maintained to avoid a reduction in capacity due to shared influence zones. The mooring line force is drawn so that helical piles "aa" and "ab" are in tension and helical piles "ba" and "bb" are in compression. If β is between 0° and 90° for all piles, the capacity of the individual helical piles can be found using the following equations.

(30) $$F_{pile\_aa} = \left[Q_{uplift}\sin(\alpha)\right]\cos(\beta) + Q_{lat}\cos\left(\alpha \times \frac{90-\beta}{90}\right)$$

(31) $$F_{pile\_ab} = \left[Q_{uplift}\sin(\alpha)\right]\sin(\beta) + Q_{lat}\cos\left(\alpha \times \frac{90-\beta}{90}\right)$$

(32) $$F_{pile\_ba} = \left[Q_{compressive}\sin(\alpha)\right]\cos(\beta) + Q_{lat}\cos\left(\alpha \times \frac{90-\beta}{90}\right)$$

(33) $$F_{pile\_bb} = \left[Q_{compressive}\sin(\alpha)\right]\sin(\beta) + Q_{lat}\cos\left(\alpha \times \frac{90-\beta}{90}\right)$$

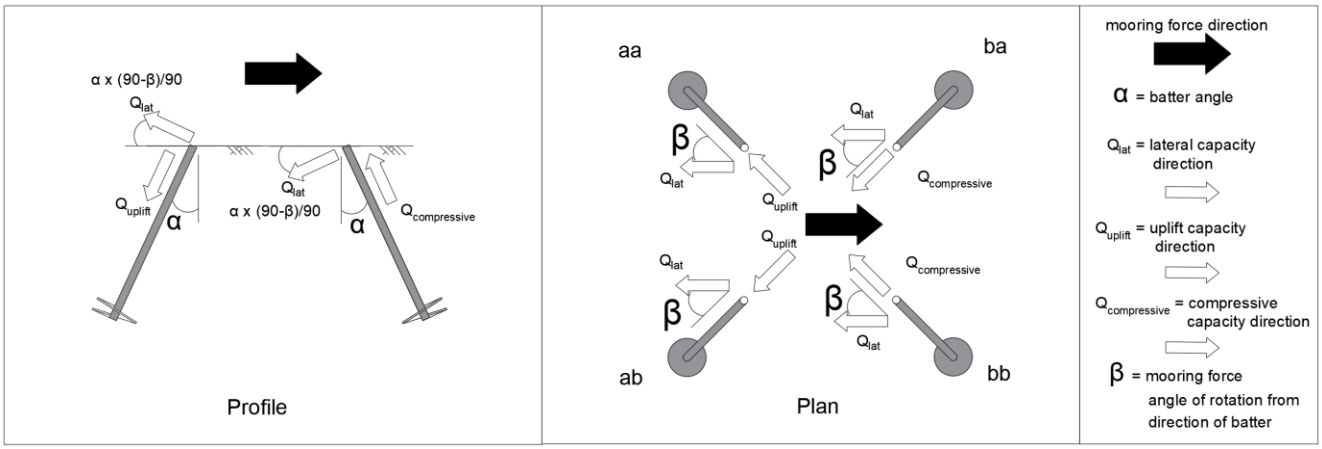

Figure 4.13. Radially Battered Pile Group with Mooring Force Out of Phase with Batter Direction.

The capacity of the group can be found as the sum of the four piles. Assuming β is 45° for every pile, the capacity of the group is estimated as 11,572 kN, which is very close to the capacity of the uniformly battered helical pile group from Figure 4.11.

Figure 4.14 presents the radially battered piles with a mooring force aligned with the batter direction of helical piles "ab" and "ba" and perpendicular to helical piles "aa" and "bb." For piles "ab" and "ba" the reduced axial and lateral capacities are contributing since β is 0°, while only the lateral capacity is contributing for piles "aa" and "bb" since β is 90°. For Figure 4.13, the capacity of the individual helical piles can be estimated using the following equations.

(34) $$F_{pile\_aa} = Q_{lat}$$

(35) $$F_{pile\_ab} = Q_{lat}\cos(\alpha) + Q_{uplift}\sin(\alpha)$$

(36) $$F_{pile\_ba} = Q_{lat}\cos(\alpha) + Q_{compressive}\sin(\alpha)$$

(37) $$F_{pile\_bb} = Q_{lat}$$

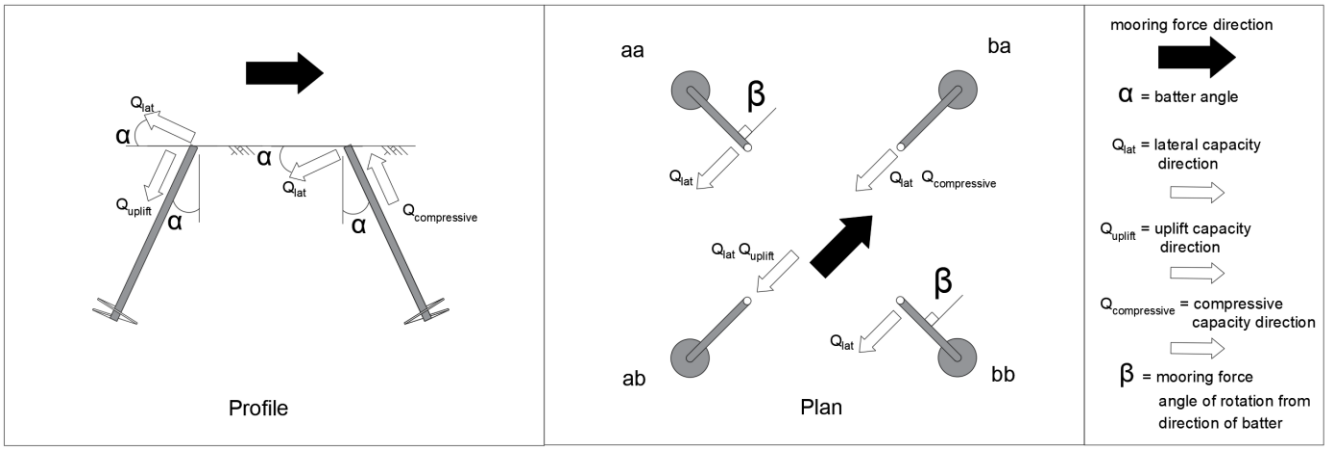

Figure 4.14. Radially Battered Pile Group with Mooring Force In Phase with Batter Direction.

The capacity of the group can be found as the sum of the four piles. For Figure 4.14, the capacity of the group is 7627 kN, which is a decrease of about 20% from Figure 4.13. The decrease in capacity between the radially battered pile in Figure 4.13 and Figure 4.14 is larger than between the uniformly battered piles Figure 4.10 and Figure 4.11. However, while the pile capacity continues to decrease for the uniformly battered piles as β increase to 90° for all piles, under similar conditions the capacity of the radially battered piles would increase as β would return to 45° for all piles.

Table 4.15. Capacity for Uniformly and Radially Battered for Helical Pile Groups.

Battering	Mooring Force Direction from Batter Direction	Group Capacity (kN)
Uniform	In Line	14,433
	Angled	11,534
	Perpendicular	3,960
Radial	Out of Phase	11,572
	In Phase	7,627

Uniformly battering helical piles maximizes the potential capacity of the pile group for a mooring line force positioned in line with the battering, shown in Table 4.15. This layout is ideal

for a single-line system, where the catenary mooring line force is designed to be in the same direction. In a multiline system, the capacity of a uniformly battered pile group will decrease as the mooring line force changes directions. A uniformly battered group has slightly greater maximum capacity than a radially battered helical pile group, the conditions of which are shown in Figure 4.10 and Figure 4.13 respectively. However, the radially battered group maintains more capacity than the uniformly battered pile group as the mooring force rotation angle changes to generate the smallest capacity, shown in Figure 4.12 for uniform battering and in Figure 14.4 for radial battering. The radially battered helical pile group layout should be considered over a uniformly battered layout for a multiline anchor design.

4.4 Helical Pile Installation Torque Estimation

This section presents results from predicting installation torque for single helical piles and individual piles in helical pile groups. Using the CPT correlation method from Davidson et al. (2019), installation torque was predicted for each pile size designed in Section 4.1 and 4.2, where the installation depth is equal to the length of the central shaft.

Table 4.15 presents the maximum torque needed for installation in each load case for the vertically installed single helical piles, and vertically installed individual piles in the 2x2 and 3x3 pile groups. Installation torque was only estimated for vertically installed piles to isolate comparisons in installation torque to pile size. In Table 4.16, the helix diameter is presented in addition to the installation depth and max required torque, because the total torque prediction is largely reliant on the helix size in shallower depths, then the shaft resistance in deeper depths. From Table 4.16 a) the longer and wider piles, for SS-M and SS-S cases, require a higher installation torque, where the SB-M case requires a much smaller torque. Looking at the smaller piles in part b) and c) the maximum installation torque is even smaller. Figure 4.16 presents max

installation torque versus helical pile length. From this figure, there is a clear, nonlinear correlation to increasing helical pile size and increasing installation torque. This clean relationship is represented by the system of equations from Davidson et al. (2019) for the specific soil properties and pile geometry specifications.

Table 4.16 Torque Predictions at Installation Depth for a) Single Piles, b) Pile Group 2x2, c) Pile Group 3x3 – for all Load Cases for Round-Shaft, Vertically Installed Piles in Sand.

a) Single Pile				
Platform Type	Semi Submersible		Spar Buoy	
Mooring Setup	Multi-Line	Single-Line	Multi-Line	Single-Line
Helix Diameter (m)	2.68	2.84	1.84	2.35
Installation Depth (m)	13.4	14.2	9.2	11.8
Max Required Torque (MN-m)	2.52	3.11	0.70	1.57

b) Pile Group 2x2				
Platform Type	Semi Submersible		Spar Buoy	
Mooring Setup	Multi-Line	Single-Line	Multi-Line	Single-Line
Helix Diameter (m)	1.69	1.79	1.16	1.48
Installation Depth (m)	8.5	9.0	5.8	7.4
Max Required Torque (MN-m)	0.55	0.65	0.15	0.35

c) Pile Group 3x3				
Pile Capacity (kN)	Semi Submersible		Spar Buoy	
Platform Type	Multi-Line	Single-Line	Multi-Line	Single-Line
Helix Diameter (m)	1.29	1.37	0.88	1.13
Installation Depth (m)	6.5	6.9	4.4	5.7
Max Required Torque (MN-m)	0.22	0.26	0.06	0.14

Installation torque with depth is shown in Figure 7.16 for a single pile, Figure 7.17 for an individual pile in the 2x2 pile group, and Figure 7.18 for an individual pile in the 3x3 pile group. These figures illustrate how the installation torque increases with depth as the pile shaft contributes more resistance. The installation torque is different for varying pile shaft diameters at the same depth, which indicates how installation torque was not just estimated as a function of depth, but also shaft diameter. Wider piles require more torque to install than thinner helical piles regardless of the installation depth.

In terms of ease of installation, the required installation torque for the single helical piles is much larger than what current commercial drive heads can produce, about 0.68 meganewton meters (MN-m) or about 0.5 million foot-lbs (M. Conte, personal communication, September 20, 2019). Only the installation torque estimated for the SB-M load case is close to this 0.68 MN-m threshold. With current technology, the single helical piles for are not able to be installed. However, the helical piles designed for pile groups require much less torque to fully install. The largest torque needed to install a pile in a pile group is about 0.65 MN-m, which is about 7% less than the torque needed for the SB-M single helical pile.

As presented in Section 4.2, the smaller helical piles designed for pile groups use more material as a single pile designed for the same load case, but since they require less torque to install, these smaller helical piles may be a better contender as an anchor for FOWT with current torqueing technology.

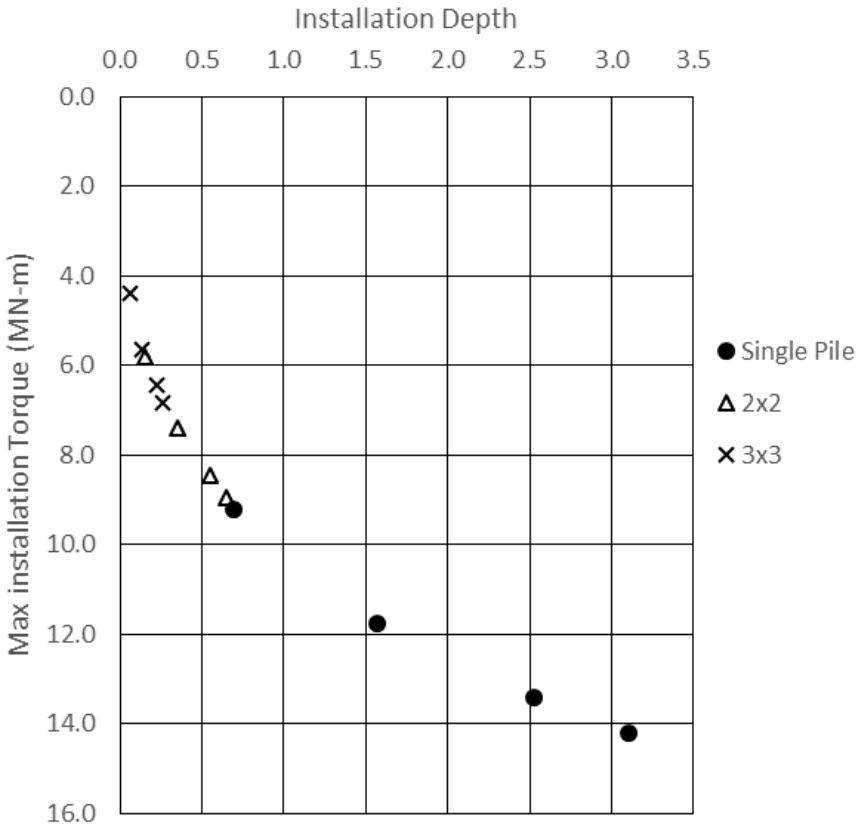

Figure 4.15 Maximum Required Installation Torque versus Helical Pile Shaft Length.

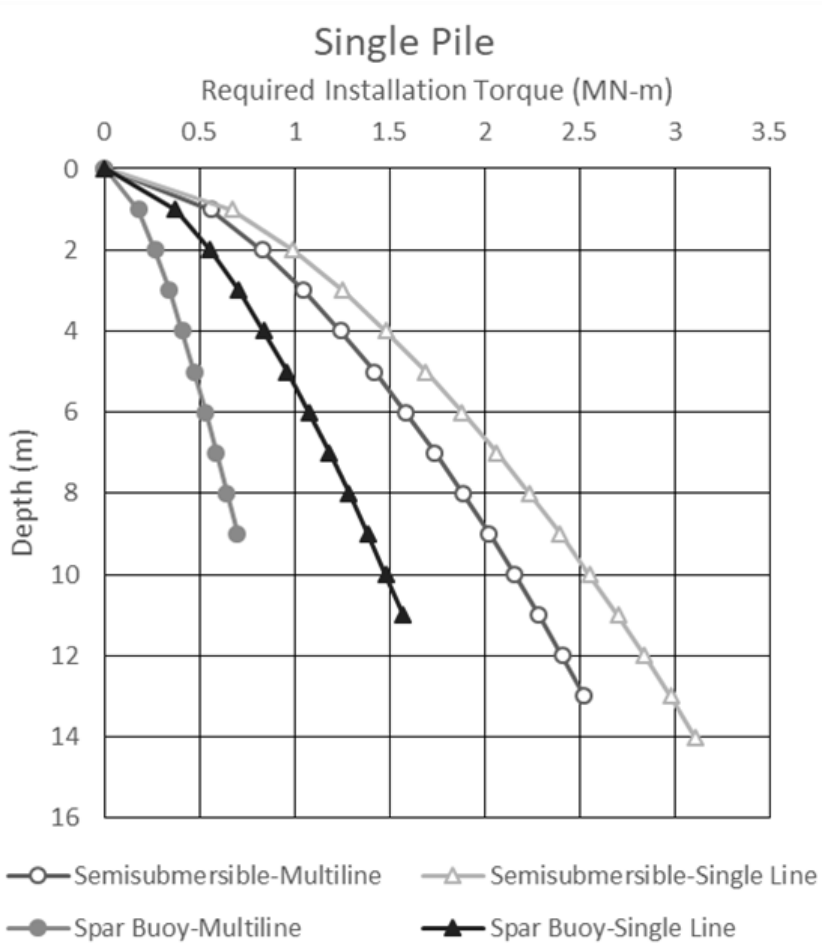

Figure 4.16 Installation Torque with Depth for Vertical Single Piles.

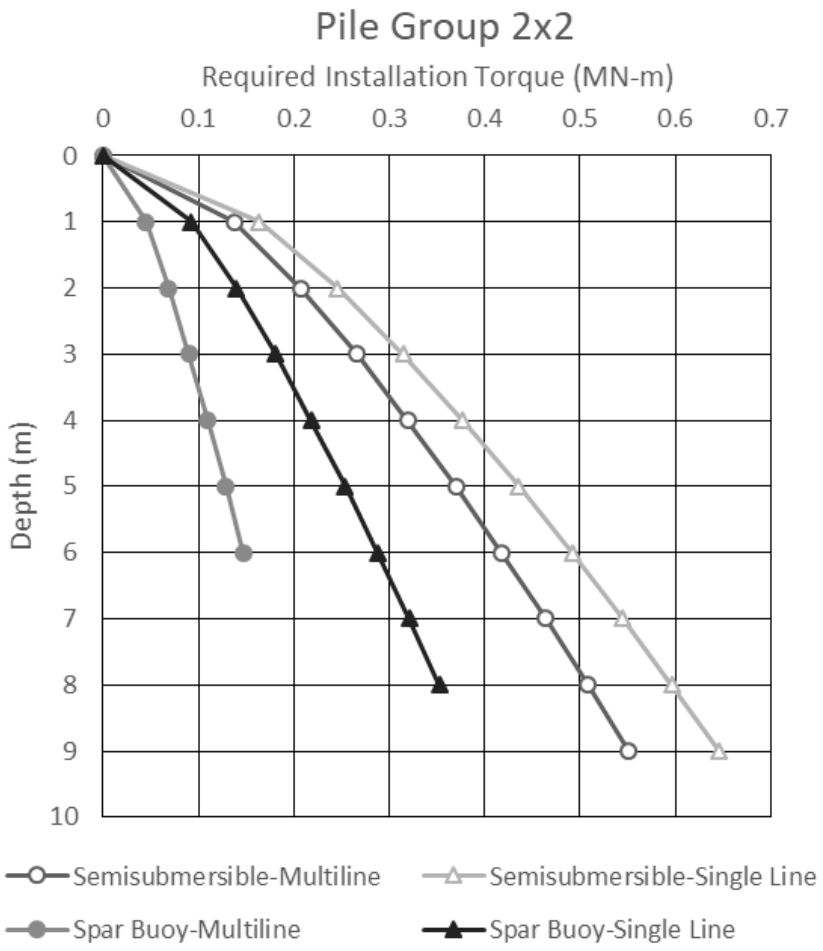

Figure 7.17 Installation Torque with Depth for Vertical 2x2 Pile Group.

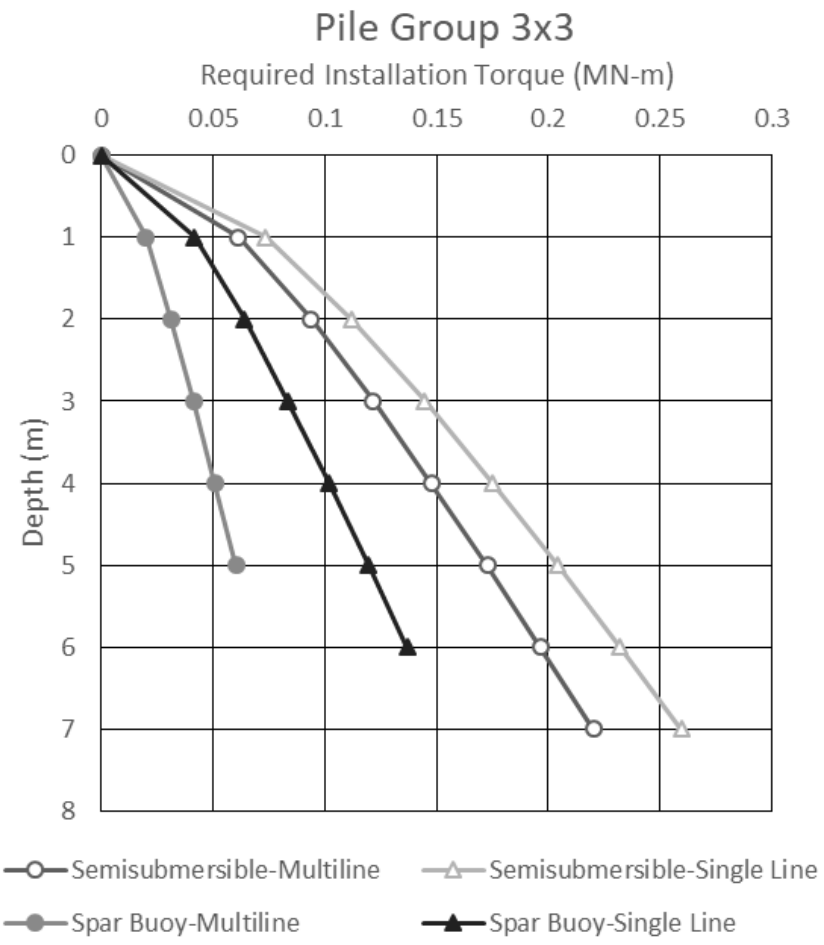

Figure 7.18 Installation Torque with Depth for Vertical 3x3 Pile Group.

CHAPTER 5: SUMMARY AND CONCLUSION

5.1 Summary

This thesis presents the methods and results from helical pile foundations designed for offshore deep-water applications as anchors for floating offshore wind systems in clay and sandy soils. Helical piles were designed for four load cases consisting of a combination of semisubmersible and spar buoy platforms with multiline and single-line catenary mooring systems (i.e., horizontal loading). Design loads were chosen from simulations of the platforms supporting a 5 MW turbine and mooring systems (Fontana 2019) under specific environmental conditions and a factor of safety of 2 was applied. The environmental setting consisted of extreme operating wind, wave and current conditions, and medium dense sand and soft clay developed to represent offshore sand and clay soils. Helical pile geometry was designed using common industry proportions among length, shaft diameter and helix geometry.. For each load case, a single helical pile, a group of 4 helical piles in a 2x2 square configuration, vertical and battered, and a group of 9 helical piles in a 3x3 square configuration, vertical and battered, was designed. Battered groups were angled 25 degrees from vertical.

The design process started with determining the appropriate lateral capacity each helical pile must have for each load case. Since the catenary mooring line produces a lateral load, the resistance needed from vertically installed piles is isolated to the lateral capacity. For piles battered away from the direction of the mooring line, the resistance comes from a combination of the lateral and uplift capacity. The lateral capacity for all pile configurations is the limiting capacity. API procedures for calculating lateral bearing capacity were used for both soil types to back calculate the pile geometry required to produce the design lateral capacity for each load case and pile configuration.

Single vertically installed suction caissons were designed and compared to single and groups of helical piles. Suction caissons were designed using a $L/D_S = 3$ and wall thickness of $t = D_S/144$. Lateral capacity was calculated using the same methods as helical piles. Axial capacity was not calculated for suction caissons.

Axial capacity of the helical pile was calculated for each load case, pile configuration and soil type using Terzaghi's bearing capacity equations. Axial capacity, which includes uplift and compressive capacity, used soil properties and designed pile geometry. Weight of the piles was also calculated. The installation torque was estimated using a CPT method developed by Davidson et al. (2018). The method used correlations between helical pile installation torque and CPT cone resistance data in sand to develop a set of equations to predict the installation torque required for a desired pile geometry. Installation torque was estimated with depth for each vertically installed helical pile, where the maximum torque occurred at the designed depth of installation, equal to the full pile shaft length.

5.2 Conclusions

The design results for a single helical pile showed, as expected, that the smallest dimensions to achieve a specified lateral capacity is for piles in the medium dense sand versus the soft clay. The medium dense sand is stiffer and has greater shear resistance than the soft clay and therefor requires a smaller pile to generate the same lateral capacity to resist the mooring force. For the four load cases considered, the smallest helical pile required was for the spar buoy platform with a multiline, catenary mooring system in the medium dense sand because the mooring force is smallest for this case. A smaller pile size not only reduces material but decreases the amount of torque required for installation, because of a smaller shaft and helical plate diameter and shallower installation depth. Compared to suction caissons designed for the same environmental and load

conditions, helical piles use less material and therefore are more efficient in terms of a normalized capacity to weight ratio. For catenary line systems the helix of a vertically installed helical pile does not contribute to lateral load resistance but it does provide a means for potentially quieter installation compared to driven piles.

The helical pile design results for vertical pile groups indicate that pile size decreases in proportion to the resistance-displacement equations used in the API method for calculating lateral capacity. The battering of groups of helical piles slightly reduced the helical pile size; for large scale application this reduction in size would be significant in terms of material cost. Even though the individual helical piles are smaller, the net weight of the vertically installed helical pile groups are more than a single pile for the same load case. These smaller piles, however, require much smaller installation torques, making them easier to install and may decrease installation cost.

In terms of suggested future work, since this study was isolated to the design of helical pile foundations, small scale physical model testing (laboratory or field) of helical piles and helical pile groups consisting of lateral and axial load tests and measurement of installation torque is needed to confirm the numerical results of this thesis. Additionally, a cost analysis of the manufacturing and installation process of helical piles, helical pile groups and suction caissons for FOWT applications is needed to fully compare the use of these foundation methods and to quantify how advantageous helical piles would be. The technology needed to install a helical pile in deep offshore conditions does not currently exist and thus direct comparison of installation cost comparison with suction caissons is not possible. Such a cost comparison, comparing the installation times of helical piles and suction caissons would be valuable. This study did not consider how the mooring line would be secured to a group of helical piles, so the design of a connection method is needed.

This thesis considers a wide range of variables, like platform type, mooring systems, soil type and pile configuration, to give a preliminary evaluation of the conditions and what helical piles would be most valuable for FOWT application. The thesis was isolated to catenary mooring systems, and semi-taut and taut mooring systems were not considered in the scope of this thesis because models and resulting loads from these mooring conditions were not available. Since helical piles have a larger axial capacity than lateral capacity, it is suggested that load conditions with semi-taut and taut mooring systems be analyzed. Additional studies focused on understanding specific elements of deep offshore helical pile installation and further analysis of radially battering pile groups would be beneficial for justifying helical piles as a potential method for FOWT anchoring.

REFERENCES

DAVIDSON, C., AL-BAGHDADI, T., BROWN, M.J., KNAPPETT, J., BRENNAN, AUGARDE, C.E., A., COOMBS, W.M., WANG, L., RICHARDS, D., BLAKE, A. & BALL, J. (2018) A modified CPT based installation torque prediction for large screw piles in sand. 4th International Symposium CPT'18 - Cone Penetration Testing. 21-22 June 2018, Delft, Netherlands. CRC Press. pp. 255-261. ISBN 9780429000485.

Fontana CM, Hallowell ST, Arwade SR, et al. Multiline anchor force dynamics in floating offshore wind turbines. *Wind Energy*. 2018;1–14.

Fontana, C., 2019. A MULTILINE ANCHOR CONCEPT FOR FLOATING OFFSHORE WIND TURBINES.

US Department of Energy, "2018 Offshore Wind Technologies Market Report," 2019.

Principle Power Inc. "WindFloat – Stability," 2019.

Turkel, T. "Competition makes UMaine think bigger about its offshore wind project." Portland Press Herald, October 2019.

American Petroleum Institute, "Recommended Practice for Design and Analysis of Station keeping Systems for Floating Structures," 2005.

Vryhof, *Anchor manual: the guide to anchoring*. 2010.

International Renewable Energy Agency, "Floating Foundations: A Game Changer for Offshore Wind Power," 2016.

Lutenegger, A, J. 2011. Historical Development of Iron Screw-Pile Foundations: 1836-1900. Int. J. for the History of Eng. & Tech., Vol. 81 No. 1.

Deep Foundations Institute, "Introduction to Helical Piles and Helical Anchors," 2019.

C. Mone, M. Hand, M. Bolinger, J. Rand, D. Heimiller, and J. Ho, "Cost of Wind Energy Review," 2015.

Lutenegger, A. J. 2018. Axial Uplift of Square-Shaft Single-Helix Helical Anchor Groups in Clay. Proceedings IFCEE Orlando, Florida.

Lanyi-Bennett, S. A., Deng, L. 2019. Axial load testing of helical pile groups in glaciolacustrine clay. Can. Geotech. J. 56: 187-197.

Whitaker, T. 1957. Experiments with model piles in groups. Geotechnique, 7(4): 147-167.

Pouos. H. G., and Davis, E. H. 1980. Pile Foundation Analysis and Design. Wiley, New York.

Hannah, A., Ghaly, A. 1994. Ultimate pullout resistance of groups of vertical anchors. Can. Geotech. J. 31, 673-682.

Perko, H. 2009. Helical Piles: A Practical Guide to Design and Installation. Wiley, New York.

Hoyt, R. M., and Clemence, S. P. 1989. Uplift capacity of helical anchors in soil. Proc. of the 12th Int. Conf. on Soil Mechanics and Foundation Engineering. Rio de Janeiro, Brazil.

Byrne, B. W. and Houlsby, G. T. 2015. Helical piles: an innovative foundation design option for offshore wind turbines. Phil. Trans. R. Soc. A, 373.

British Standards Institution. 2015. BS 8004-2015. Code of practice for foundations. Milton Keynes: BSI.

American Petroleum Institute, "Recommended Practice for Planning, Designing and Constructing Fixed Offshore Platforms – Load and Resistance Factor Design," 1993.

Lutenegger, A, J. 2019.Design of Helical Piles and Anchors in Soil – Quick Guide Ver. 1.2. Int. Society for Helical Foundations.

U.S. Navy Design Manual DM-7.02. 1986. Foundations and Earth Structures.

Singh, T., Arora, V. K. 2017. INFLUENCE OF PILE INCLINATION ON BATTER PILE GROUPS SUBJECTED TO LATERAL LOADING IN SAND. Proceedings of 29thResearch World International Conference, Las Vegas, USA. 13-15.

DAVIDSON, C., BROWN, M.J., CERFONTAINE, B., KNAPPETT, J.A., BRENNAN, A.J., AL-BAGHDADI, T., AUGARDE, C., COOMBS, W., WANG, L., BLAKE, A., RICHARDS, D.J. & BALL, J.D. Feasibility of screw piles for offshore jacket structures. Geotechnique. Accepted subject to revision 20/02/19. Re-submitted 29/10/19.